The regime of aerosol asymmetry parameter over Europe, Mediterranean and Middle East based on MODIS satellite data: evaluation against surface AERONET measurements

M. B. Korras-Carraca[1], N. Hatzianastassiou[2,*], C. Matsoukas[1], A. Gkikas[2], C. D. Papadimas[2]

[1]{Department of Environment, University of the Aegean, 81100 Mytilene, Greece}

[2]{Laboratory of Meteorology, Department of Physics, University of Ioannina, 45110 Ioannina, Greece}

Correspondence to: N. Hatzianastassiou (nhatzian@cc.uoi.gr)

Abstract

Atmospheric particulates are a significant forcing agent for the radiative energy budget of the Earth-atmosphere system. The particulates' interaction with radiation, which defines their climate effect, is strongly dependent on their optical properties. In the present work, we study one of the most important optical properties of aerosols, the asymmetry parameter (g_{aer}), in the region comprising North Africa, the Arabian peninsula, Europe, and the Mediterranean basin. These areas are of great interest, because of the variety of aerosol types they host, both anthropogenic and natural. Using satellite data from the collection 051 of MODIS (MODerate resolution Imaging Spectroradiometer, Terra and Aqua), we investigate the spatio-temporal characteristics of the asymmetry parameter. We generally find significant spatial variability, with larger values over regions dominated by larger size particles, e.g. outside the Atlantic coasts of north-western Africa, where desert-dust outflow takes place. The g_{aer} values tend to decrease with increasing wavelength, especially over areas dominated by small particulates. The intra-annual variability is found to be small in desert-dust areas, with maximum values during summer, while in all other areas larger values are reported during the cold season and smaller during the warm. Significant intra-annual and inter-annual variability is observed around the Black Sea. However, the inter-annual trends of g_{aer} are found to be generally small.

Although satellite data have the advantage of broad geographical coverage, they have to be validated against reliable surface measurements. Therefore, we compare satellite-measured values with g_{aer} values measured at 69 stations of the global surface AERONET (Aerosol Robotic Network), located within our region of interest. This way, we provide some insight on the quality and reliability of MODIS data. We report generally better agreement at the wavelength of 870 nm (correlation coefficient R up to 0.47), while of all wavelengths the results of the comparison were better for spring and summer.

1 Introduction

Atmospheric aerosol particles interact with radiation, mainly the short wave (SW or solar) part of the spectrum, modifying the energy budget of the Earth-atmosphere system. The aerosol effect is either direct, through the scattering and absorption of solar radiation, and thus reducing the incoming solar radiation flux at the surface, indirect, through the modification of cloud properties, or semi-direct, due to the absorption of solar radiation and consequent modification of the atmospheric temperature profile, convection, and cloud properties (e.g. Graβl, 1979; Hansen, 1997; Lohmann and Feichter, 2005).

The interaction of particles with the solar flux, which defines their climate role, strongly depends on their optical properties (Hatzianastassiou et al., 2004; 2007), which cannot be covered globally by surface in situ measurements. Besides the aerosol optical depth (AOD), one of the most important optical properties of atmospheric particles, which is used in radiative transfer, climate, and general circulation models, is the asymmetry parameter (g_{aer}). The asymmetry parameter describes the angular distribution of the scattered radiation and determines whether the particles scatter radiation preferentially to the front or back. The globally available satellite based AOD data are considered to a great extent as reliable and adequate, due to significant developments in surface and satellite measurements during the last two decades, and particularly the arrival of MODIS in 2000, which is regarded as one of the most reliable datasets (Bréon et al., 2011; Nabat et al., 2013). On the other hand, despite the important role of the asymmetry parameter, relevant global coverage data are measured only for the few last years, or are available in long-term aerosol climatologies such as Global Aerosol Data Set (GADS, Koepke et al. 1997) and Max Planck Aerosol Climatology (MAC, Kinne et al., 2013). Even so, asymmetry parameter data are usually examined for regions with limited geographical extent and temporal coverage (Di Iorio et al, 2003), without intercomparison between alternative data platforms.

The goal of the present work is the study of the spatiotemporal distribution of the aerosol asymmetry parameter, using the most recent data from MODIS (MODerate resolution Imaging Spectroradiometer, collection 051). Emphasis is given to the comparison between the provided MODIS data and respective reliable surface measurements of the global AERONET, in order to gain insight on the quality of the former.

For this study we focus on the region defined by latitudes 5°N to 70°N and longitudes 25°W to 60°E, including North Africa, the Arabian peninsula, Europe, and the greater Mediterranean basin (Fig. 1). This area is selected because it is of particular scientific interest due to the simultaneous presence of a variety of particles, both natural and anthropogenic (e.g. desert dust, marine, biomass burning, anthropogenic urban / industrial pollution) as shown in previous studies (Lelieveld et al., 2002; Smirnov et al., 2002; Sciare et al., 2003; Pace et al., 2006; Lyamani et al., 2006; Gerasopoulos et al.,2006; Engelstaedter et al., 2006; Satheesh et al., 2006; Kalivitis et al., 2007; Rahul et al., 2008; Kalapureddy et al., 2009; Alonso-Pérez et al., 2012; Zuluaga et al., 2012; Kischa et al., 2014) which makes this area ideal for aerosol studies. The presence of a variety of aerosols in the area is due to the fact that two of the largest deserts of the planet are partly included in our area of interest, i.e. the Arabian desert and the Sahara, while one finds also significant sources of anthropogenic pollution from urban and industrial centres, mainly in the European continent. Moreover, our area of interest and primarily its desert areas are characterised by a large aerosol load (large optical depth, Remer et al. 2008; Ginoux et al. 2012). In addition, significant regions in this area, more specifically the Mediterranean basin and North Africa, are considered climatically sensitive, since they are threatened by desertification (IPCC, 2007; 2013). Finally, one more reason for the selection of study area is that the present study complements previous ones made by our team (e.g. Papadimas et al., 2008, 2012; Hatzianastassiou et al., 2009) analysing other key aerosol optical properties, namely AOD, for the same region. This is the first study (to our knowledge) that focuses on asymmetry parameter over a geographically extended area, while at the same time compares satellite with ground-station data.

2 Data

Before presenting the data used in this study, a short introduction of the parameter studied is given here for readers more or less unfamiliar with it. The asymmetry parameter (or factor) is defined by:

$$g = \frac{\overline{\omega}_1}{3} = \frac{1}{2}\int_{-1}^{1} P(\cos\Theta)\cos\Theta d\cos\Theta \qquad (1)$$

where P is the phase function, which represents the angular distribution of the scattered energy as a function of the scattering angle Θ and it is defined for molecules, cloud particles, and aerosols. The phase function can be expressed using the Legendre polynomials $\overline{\omega}_l$ (see Liou, 2002) and $\overline{\omega}_1$ in Eq. (1) stands for l=1. The asymmetry parameter is the first moment of the phase function and it is an important parameter in radiative transfer. For isotropic scattering, g equals zero, which is the case for Rayleigh molecular scattering. The asymmetry parameter increases as the diffraction peak of the phase function sharpens. For Lorenz-Mie type particles, namely for aerosols and cloud droplets, the asymmetry parameter takes positive values denoting a relative strength of forward scattering, with values increasing with particle size. It can also take negative values if the phase function peaks in backward directions (90-180°). The phase function along with the extinction coefficient (or equivalently the optical depth) and the single scattering albedo, constitute the fundamental parameters that drive the transfer of diffuse intensity (Joseph et al., 1976). The asymmetry parameter itself is a simple expression of the phase function (being its first moment) and it is used in many radiative transfer and climate models. Hence, the importance of aerosol asymmetry parameter is easily understood for enabling computations of aerosol radiative properties and effects (e.g. forcings).

Daily data of the aerosol asymmetry parameter (g_{aer}) are used for the needs of this work. In order to achieve the largest geographical coverage of the studied region, we employ satellite data from the MODIS-Terra and MODIS-Aqua datasets. These data are compared with in-situ measurements at stations of the AERONET. We provide a detailed description of the utilised data in the following sections.

2.1 Satellite MODIS Terra and Aqua data

MODIS is an instrument (radiometer) placed on the polar-orbiting satellites of NASA (National Aeronautics and Space Administration) Terra and Aqua, 705 km from the Earth, in the framework of the Earth Observing System (EOS) programme. Terra was launched on 18 December 1999, while Aqua was launched on 4 May 2002. The two satellites are moving on opposite directions and their equatorial crossing times are at 10:30 (Terra) and 13:30 (Aqua). MODIS is recording data in 36 spectral channels between the visible and the thermal infrared (0.44 – 15 μm), while its swath width is of the order of 2330 km, which results in almost full planetary coverage on a daily basis.

Aerosol properties are monitored in 7 spectral channels between 0.47 and 2.13 μm and final results are derived through algorithms developed for aerosol quantities both over land and ocean (Kaufman et al., 1997; Tanré et al., 1997; Ichoku et al., 2002; Remer et al., 2005). MODIS data are organised in "collections" and "levels". Collections comprise data produced by similar versions of the inversion algorithms, with the recent collection "051" including also outputs from the "Deep Blue" algorithm. Levels are characterised by data of different quality analysis and spatial resolution.

In this study we use daily MODIS data for the asymmetry parameter (g_{aer}) provided on an 1°x1° grid (namely 100x100 km), from Collection 051, Level 3. These data were measured at wavelengths 470, 660, and 870 nm, only over oceanic regions, since they were derived through the algorithm "Dark Target" over ocean. The period of analysis stretches from 24-2-2000 to 22-9-2010 for MODIS-Terra and from 4-7-2002 to 18-9-2010 for MODIS-Aqua.

The MODIS C051 g_{aer} data are a derived product of the MODIS algorithm over ocean. This MODIS algorithm (http://modis.gsfc.nasa.gov/data/atbd/atbd_mod02.pdf, Remer et al., 2006) retrieves as primary products the AOD at 550 nm, the Fine (Mode) Weighting (FW, also known as fraction of fine-model aerosol type, FMF) and the Fine (f) and Coarse (c) modes used in the retrieval, along with the fitting error (ε) of the simulated spectral reflectance. The algorithm reports additional derived parameters, such as the effective radius (r_e) of the combined size distribution, the spectral total, fine and coarse AODs or the columnar aerosol mass concentration. Among them, g_{aer} is also derived and reported at seven (7) wavelengths, 470, 550, 660, 860, 1200, 1600 and 2120 nm. The derived parameters are calculated (Levy et al., 2013) from information contained within the look-up table (LUT) and/or other retrieved products. For example, knowing the resulting total AOD and FMF, and which aerosol types were selected (or assumed), one can go back to the LUT, and recover additional information about the retrieved aerosol, such as the g_{aer}. Hence, it should be noted that the derived g_{aer} product is dependent on the used aerosol models (modes), since the algorithm is based on a LUT approach, assuming that one fine and one coarse lognormal aerosol modes can be combined with appropriate weightings to represent the ambient aerosol properties over the target (spectral reflectance from the LUT is compared with MODIS-measured spectral reflectance to find the "best" – least squares – fit, which is the solution to the inversion). In the C051 algorithm there are four fine modes and five coarse modes, for which the spectral (at the aforementioned 7 wavelengths) aerosol asymmetry parameter values are given in Remer et al (2006).

We also used Level 3 daily Ångström exponent data from MODIS-Aqua C051, and also spectral aerosol optical depth data from MODIS-Aqua C006 datasets, from which we computed C006 Ångström exponent. These data were used to assess the validity of g_{aer} data and their temporal tendencies, as discussed in section 3.2.3.

2.2 Ground based AERONET data

AERONET (AErosolROboticNETwork) is a global network of stations focused on the study of aerosol properties. AERONET currently encompasses about 970 surface stations (number continuously evolving) equipped with sun photometers of type CIMEL Electronique 318 A (Holben et al., 1998), which take spectral radiation flux measurements.

The optical properties of aerosols are extracted through the application of inversion algorithms (Dubovik and King, 2000). Data are provided on three levels (1.0, 1.5, and 2). In the present work, we use the most reliable cloud-screened and quality assured Level 2 data. AERONET calculates the asymmetry parameter at wavelengths 440, 675, 870, and 1020 nm. We employ daily Level 2 asymmetry parameter data from 69 stations (Fig. 1), contained in our study area (N. Africa, Arabian peninsula, Europe). We choose only coastal stations, in order to maximize the coexistence of satellite marine g_{aer} data with surface data. Also, in order to compare corresponding data between the satellite and station platforms, we perform comparison only for the 440, 675 and 870 nm.

3 Satellite based results

3.1 Geographical distributions

The spatial distribution of annual mean values of g_{aer} is given in Fig. 2 separately at the wavelengths 470, 660 and 870 nm. The values are averages over the common period between Terra and Aqua, namely 4 July 2002 till 18 September 2010. A significant spatial variability is evident, with MODIS-Terra values varying within the ranges 0.63 - 0.76, 0.57 – 0.75, and 0.55 – 0.74, at 470, 660 and 870 nm, respectively. The results exhibit a decreasing tendency of g_{aer} with increasing wavelength, consistent with the theory. Similar results are also obtained from MODIS-Aqua, but with slightly smaller values than Terra by up to 0.02 on average. More specifically, the corresponding ranges of wavelengths are 0.63 - 0.75, 0.57 – 0.73, and 0.55 – 0.73. The smaller Aqua than Terra g_{aer} values could be attributed to smaller sizes of aerosols in midday than morning, corresponding to passages of Aqua and Terra, respectively, associated with lower relative humidity values and shrinking of aerosol particles. It should be reminded that the ability of atmospheric aerosol to absorb water affects the particle size (hygroscopic growth), as described by Köhler theory in the early 20th century. It is also well known that relative humidity significantly affects aerosol optical properties (e.g. Pilinis et al., 1996; Kondratyev, 1999), namely AOD, single scattering albedo and g_{aer}, by modifying the aerosol liquid water content, size and hence extinction coefficient and refractive indices. More specifically, aerosol asymmetry parameter increases with increasing aerosol size, as noted in sect. 2. Such diurnal variation has been also reported for AOD (Smirnov et al., 2002; Pandithurai et al., 2007), but either decreasing or increasing in the day because of the influence of other factors too, e.g. emissions or wind conditions, apart from aerosol hygroscopicity.

In general, the largest g_{aer} values (deep red colors) are observed off the coasts of West Africa (eastern tropical Atlantic Ocean) at all three wavelengths. High values are also found over the Red and Arabian Seas. These high values are due to strong dust outflows from the Saharan and Arabian deserts carrying out coarse aerosol particles (Prospero et al., 2002; Alonso-Pérez et al., 2012; Miller et al., 2008) and causing strong forward scattering. Nevertheless, the Persian Gulf region, which is surrounded by deserts, is characterized by relatively smaller g_{aer} values. More specifically, values as small as 0.69 (MODIS-Terra) and 0.67 (MODIS-Aqua) are observed in this region at 470 nm, while at the longer wavelengths (660, 870 nm) the smallest values are equal to 0.66 (Terra) and 0.64 (Aqua). The smaller g_{aer} values over the Persian Gulf can be attributed to the presence of fine aerosols, which is corroborated by the low effective radius and large fine-fraction measurements by MODIS over the Persian Gulf, compared to neighbouring areas (not shown here). These fine particles originate from the industrial activities in the Gulf countries related to oilfields or refineries (Goloub and Arino, 2000; Smirnov et al., 2002a,b; Dubovik et al., 2002).

The high g_{aer} values over the northeastern tropical Atlantic Ocean as well as west of the Iberian coasts are possibly related with the presence of coarse sea salt particles. On the other hand, the asymmetry parameter takes clearly smaller values over the Black Sea, where according to MODIS-Terra varies between 0.63 and 0.7 at 470 nm, 0.57 and 0.67 at 660 nm, and 0.55 and 0.66 at 870 nm, with the smallest values appearing over the Crimean peninsula (corresponding maximum Aqua values are smaller by 0.02). The small Black Sea g_{aer} values can be associated with industrial but also biomass burning activities in nearby countries. A region of special interest is the Mediterranean basin since it hosts a large variety of aerosols like anthropogenic, desert dust or sea salt (e.g. Barnaba and Gobbi, 2004). The MODIS results over this region show relatively small g_{aer} values, secondary to those of Black Sea, characterized by an increase from north to south, which is more evident at 660 and 870 nm. More specifically, based on MODIS-Terra, g_{aer} over the Mediterranean takes values from 0.68 to 0.74 at 470 nm, while at 670 and 870 nm it ranges from 0.64 to 0.73 and 0.62 to 0.72, respectively. According to MODIS-Aqua the g_{aer} values are slightly smaller again. The observed low values in the northern parts of the Mediterranean are probably associated with the presence of fine anthropogenic aerosols transported from adjacent urban and industrial areas in the north, especially in central Europe. In contrast, the higher g_{aer} values in the southern Mediterranean, particularly near the North African coasts, can be explained by the proximity to the Sahara desert and the frequent transport of significant amounts of coarse dust (e.g. Kalivitis et al., 2006; Hatzianastassiou et al., 2009; Gkikas et al., 2009; 2014).

The spatial distributions of climatological monthly mean g_{aer} values from MODIS-Aqua at 470 nm reveal significant differences in the range and the patterns of the seasonal variability, depending on the area (Fig. 3). Thus, in tropical and sub-tropical areas of Atlantic Ocean (up to about 30°N), where dust is exported from Sahara, g_{aer}

keeps high values throughout the year, which reach or even exceed 0.74 locally. Over the regions of Arabian and Red Seas and the Gulf of Aden, which also experience desert dust transport, larger g_{aer} values appear in the period from March to September, with a maximum in August (locally as high as 0.75-0.76). This seasonal behavior is in line with intra-annual changes of dust production over the Arabian peninsula indicated by MODIS Ångström Exponent (AE) and Deep Blue aerosol optical depth data (Ginoux et al., 2002), as well as over southwest Asia through in-situ data (Rashki et al., 2012), aerosol index from various platforms and MODIS Deep Blue AOD data (Rashki et al., 2014). Indeed, the production of dust there is relatively poor in winter, increases in March and April and becomes maximum in June and July (Prospero et al., 2002). Over the Arabian Sea, it is known that large amounts of desert dust are carried out during spring and early summer (Prospero et al, 2002; Savoie et al., 1987; Tindale and Pease, 1999; Satheesh et al., 1999). Nevertheless, according to MODIS, the seasonal variability of g_{aer} remains relatively small there in line with a small seasonal variability in MODIS Deep Blue AE data (results of our analysis, not shown here). This can be explained by the presence of sea salt coarse particles throughout the year, with which dust particles co-exist.

A greater seasonal variability exists over the Persian Gulf, where g_{aer} values are higher during spring and in particular in summer (up to 0.74 at 470 nm according to Aqua), and smaller in autumn and winter (area-minimum values smaller than 0.65). This seasonal behavior can be explained taking into account the meteorological conditions over the greater area of the Gulf; mainly in spring and summer dry northwestern winds (Shamal) blow from northwest carrying desert dust from the arid areas of Iraq (Heishman 1999; Smirnov et al. 2002a,b; Kutiel and Furman, 2003). The transport of dust is gradually decreased in autumn and reaches its minimum in winter. When the presence of desert dust is limited, a significant fraction of total aerosol load in the region consists of fine anthropogenic particles (Smirnov et al. 2002a,b), which can explain the observed relatively small g_{aer} values in autumn and winter.

In the Mediterranean basin g_{aer} exhibits a relatively small seasonal variation, with lower values tending to appear in summer and secondarily in early and late spring, in line with the stronger presence of dust in the area, transported from the Sahara desert (Gkikas et al., 2013). On the contrary, over the Black Sea, a clear seasonal cycle is apparent, with higher values in the cold period of the year and smaller in the warm one. More specifically, according to MODIS-Aqua, the values at 470 nm drop down to 0.61 in summer months whereas they reach 0.7 in January and December. This seasonality is in agreement with the summer biomass burning from agricultural activities and wildfires (Barnaba et al., 2011; Bovchaliuk et al., 2013), and the resulting abundance of fine particles.

It is also interesting to look at the geographical distribution of monthly g_{aer} values in latitudes higher than 50°N, for which annual mean values were not given in Fig. 2 because of unavailability of data for all months. Off shore northern France (English Channel) and Germany the asymmetry parameter has small seasonally constant values (note that data do not exist for January and February). In these areas, the aerosol load consists mainly of anthropogenic polluted particles, which explains the small g_{aer} values there.

In the Baltic Sea (values available from March to October) g_{aer} shows a significant spatial and temporal variability. More specifically, it is small during summer whereas it increases, locally up to more than 0.7, in March and October. The smaller summer values can be explained by the presence of fine aerosols in the Baltic Sea originating from forest fires in Europe and Russia (Zdun et al., 2011). On the contrary, in autumn the local aerosol loading consists largely of coarse marine aerosols. It is also important to note that the Baltic Sea hosts significant amounts of anthropogenic industrial and urban aerosols throughout the year, but especially in summer (Zdun et al., 2011).

In the higher latitudes of Atlantic Ocean, where the presence of maritime aerosols is dominant, we note a remarkable month by month variation of asymmetry parameter, with low values in summer (values up to 0.59) against high values (up to 0.75-0.77) in spring (March, April) and autumn (October). This difference is possibly explained by the seasonal variability of aerosol size in the northern Atlantic. Apart from the presence of coarse sea salt throughout the year, in spring and summer small particles are formed through photochemical reactions of dimethylsulphide (DMS) emitted by phytoplankton decreasing the aerosol size. Moreover during summer fine anthropogenic aerosols are transported in the region from North America (Yu, 2003; Chubarova, 2009). These result in lower g_{aer} values between May and August.

Based on MODIS-Terra, the patterns of spatial distribution are generally the same with Aqua, with slightly larger g_{aer} values. At larger wavelengths (660, 870 nm) a decrease of g_{aer} is observed, especially for its smallest values. Further details and an overall picture are given in section (3.2.1) which deals with climatological monthly mean values not at the pixel but at the regional level.

3.2 Temporal variability

3.2.1 Seasonal variability

In order to provide an easier assessment of the seasonal cycle of aerosol asymmetry parameter and its changes from one region to another, but also among the different wavelengths (470, 660 and 870 nm), the study region was divided in 6 smaller sub-regions (see Fig. 1). The average values of monthly mean climatological data of the pixels found within each sub-region's geographical limits have been computed and are given in Fig. 4, for every wavelength, both for Terra and Aqua. It appears that the seasonal cycle differs between the sub-regions, as it has been already shown in the geographical map distributions discussed in the previous section.

At 470 nm (Fig. 4i), the intra-annual variability of g_{aer} is greater over the Black Sea, where it is as large as 0.06 according to MODIS-Terra and 0.05 according to MODIS-Aqua, the north-eastern Atlantic Ocean (0.04 and 0.05 for Terra and Aqua, respectively) and the seas of North Europe (0.05 for both Terra and Aqua). In these regions, there is a tendency for smaller values during summer. More specifically, in the Black Sea the smallest g_{aer} value (0.64) is observed in June, over the seas of North Europe in July and over the north-eastern Atlantic Ocean in August. In these regions, the largest values appear in the cold period of the year. Reverse seasonality with a large seasonal amplitude is observed over the Persian Gulf, where the variability is as large as 0.08, according to both MODIS-Terra and Aqua. The seasonal cycle of g_{aer} over the Middle East exhibits a smaller range of variability (0.02 for MODIS-Terra and 0.03 for Aqua) along with a reverse seasonal variation, with maximum values in summer and minimum in winter. In the other two sub-regions (Mediterranean and eastern Atlantic Ocean) the annual range of values is small (< 0.02). It is noteworthy that in the Mediterranean Sea, there is a weak tendency of appearance of double maxima in winter and spring. The spring maximum should be associated with the presence of desert dust particles, which are transported from Sahara, mainly in the eastern Mediterranean in this season (e.g. Fotiadi et al., 2006; Kalivitis et al., 2007; Papadimas et al. 2008, Gkikas et al. 2009; Hatzianastassiou et al., 2009; Gkikas et al., 2013). There is also a similar transport of Saharan dust in the central and western

Mediterranean during summer and autumn (e.g. Gkikas et al., 2009; 2013), but then the predominance is not so clear because of the co-existence of fine anthropogenic aerosols. Regardless of the annual cycle, smaller g_{aer} values are clearly distinguished over the Black Sea and North Europe seas throughout the whole year.

At 660 nm, the g_{aer} values are lower than at 470 nm, in particular over Black Sea, North Europe and North-East Atlantic, whereas the intra-annual variability (range of g_{aer} values) increases up to 0.10 (Terra) and 0.08 (Aqua) over the Black Sea. This increase is mainly attributed to the reduction of summer values due to the strong appearance of fine aerosols in this season. Also, at 660 nm, there is a clearer double annual variation of g_{aer} over the Mediterranean Sea than at 470 nm. At 870 nm the general picture is similar to that of 660 nm though a further increase of month by month variability is noticeable.

In general, our results indicate that over the regions characterized by a strong presence of desert dust particles (eastern Atlantic and the Middle East and Mediterranean Seas) the annual range of variability of g_{aer} is smaller than in the other regions. An additional feature above regions with desert dust is the smaller decrease of g_{aer} values with increasing wavelengths. This is attributed to the lower g_{aer} spectral dependence of coarse compared to fine particles (e.g. Dubovik et al, 2002; J. Bi et al., 2011).

We should note that the MODIS-Terra and Aqua g_{aer} seasonal cycles are about similar but with generally greater larger Terra than Aqua values.

3.2.2 Inter-annual variability and changes

Figure 5 displays the geographical distribution of the slope of inter-annual trend of g_{aer} over the study region, as computed from the application of the Mann-Kendall test to time series of deseasonalized monthly anomalies of g_{aer} at 470 nm. Results are shown in units decade^{-1} for both Terra and Aqua over their common time period, namely 2002 – 2010, only if the trend is statistically significant at the 95% confidence level. We also performed the same analysis for the 660 and 870 nm (not shown), with similar results to the 470 nm wavelength.

In general, the estimated changes are relatively small. Terra produces widely statistically significant positive trends, showing that during the period of interest, the asymmetry parameter increased over the examined area, with very few exceptions. The results from Aqua are statistically significant at considerably fewer cells, but also give a few points with decreasing g_{aer}. Based on Terra data, the stronger increases are observed in the eastern and southern Black Sea, as well as over the Baltic and Barents Seas. According to MODIS-Aqua, negative trends are found over few Atlantic Ocean cells. Both Aqua and Terra report increases of g_{aer} over the Persian Gulf, the Red Sea, South Black Sea, East Mediterranean, the coast of the Iberian Peninsula, and some coastal areas of West Africa. The differences encountered between the Terra and Aqua g_{aer} trends may be attributed to the different time of passage of each satellite platform carrying the same MODIS instrument, given that everything else is the same. Nevertheless, they may more probably be the result of calibration differences between the two MODIS sensors. It is known that there is a degradation of MODIS sensor (Levy et al., 2010; Lyapustin et al., 2014) impacting time series of MODIS products. More specifically, it is also known that Terra suffers more than Aqua from optical sensor degradation. These calibration issues are known to affect MODIS AOD retrievals, producing an offset between Terra and Aqua, and they are also expected to affect aerosol asymmetry parameter, which is probably more sensitive to such calibration uncertainties than AOD. In this sense, the results of Fig. 5 shown here are not to be taken as truth but rather they are given as a diagnostic of a problematic situation with MODIS aerosol asymmetry parameter inter-annual changes. Such calibration issues are expected to be addressed, at least partly, in the new Collection 006 products. Nevertheless, a preliminary comparison between MODIS Aqua C051 and C006 Ångström exponent (AE), which is another common aerosol parameter strongly dependent on size, using data for the 550-865 pair of wavelengths spanning the period 2002-2010, does not reveal significant modifications in geographical patterns of AE inter-annual changes.This puts some confidence on the C051 g_{aer} results given in the present study. The results of this analysis are presented in detail in the next sub-section (3.2.3).

The overall g_{aer} changes of Fig. 5 may hide smaller timescale variations of g_{aer}, which are obtained by the time-series shown in Fig. 6. Results are given for the 7 sub-regions defined previously, at the three different wavelengths and for Terra and Aqua separately. A general pattern is the decrease of g_{aer} values with increasing wavelength, in particular from 470 to 660 nm. The largest month to month and year to year variation is for Black Sea (Fig. 6i). Relatively large variability is also found in the sub-regions of NE Atlantic (6v), North Europe (6vi) and the Persian Gulf (6vii). On the contrary, small variability is noticed in the eastern Atlantic, where systematic dust outflows from Sahara take place leading to consistently high values of g_{aer}. There are also some other interesting patterns, like the significant drop of g_{aer} with wavelength in areas characterized by the presence of fine aerosols, namely the Black Sea, North Europe and the Persian Gulf (Figs, 6i,vi,vii, respectively). The specific patterns of inter-annual changes of g_{aer} are suggested by both Terra and Aqua, though a slight overestimation by Terra is again apparent in this figure. The obtained results of our analysis are meaningful and in accordance with the theory, underlining the ability of satellite observations to reasonably capture the g_{aer} regime over the studied regions.

3.2.3 Possible uncertainties of MODIS aerosol asymmetry parameter

The MODIS aerosol asymmetry parameter is not a direct retrieval product of the MODIS retrieval algorithm, but it is rather a derived by-product. Since this parameter is dependent on aerosol modes used and relative weights, it is understood that there can be uncertainties associated with it. Therefore questions may arise about the validity of g_{aer} and their spatial and temporal patterns presented in the previous sub-sections. Given that, as already mentioned, it is an aerosol optical parameter that is valuable and highly required by radiative transfer and climate models, it is worth assessing it through comparison against another more common aerosol size parameter, namely the C051 MODIS Ångström exponent at the 550-865 nm wavelength pair ($AE_{550-865}$) over ocean, which is an evaluated MODIS aerosol size product (Levy et al., 2010) that is extensively used in literature. Figure 7a, displays the geographical distribution of long-term average AE for the whole study period, i.e. 2002-2010. In this figure, the northernmost areas are blank with respect to g_{aer} (Fig. 7a) because there are no data during winter and a long-term average would be biased. The main geographical patterns in Fig.7a are in line with those of asymmetry parameter (Fig. 2). For example, note the high AE values in the Black Sea (between about 1.3 and 1.8, yellowish-reddish colors), indicative of fine aerosols, the relatively high values in the Mediterranean Sea (between about 0.7 and 1.2, greenish-yellowish colors) and the low values (0.1-0.4, deep bluish colors) off the western African coasts corresponding to exported Saharan dust. Over the same areas, g_{aer} takes inverse low and high values, for example smaller than 0.65 over the Black Sea and larger than 0.7-0.75 off the western African coasts (Figs 2ii-b and 2iii-b), indicating the predominance of fine and coarse aerosols respectively, in accordance with AE. The consistency between g_{aer} and AE data is shown by the strong anti-correlation between the MODIS $AE_{550-865}$ and g_{aer} data at 660 and 870 nm, shown in Figures7b and 7c, respectively. It should be noted that correlation coefficients are computed from any available data pairs, i.e. available data for both g_{aer} and $AE_{550-865}$ at a given pixel and day. Note that there are no blank areas in Figs 7b and 7c, opposite to Fig. 7a, because as there are both AE and g_{aer} data for all but winter months, correlation coefficients can be calculated for these regions (Figs. 7b, 7c). Strong negative correlation coefficients, larger than 0.7 and 0.8 in Figs 7b and 7c, respectively, relate inversely high g_{aer} values with low AE ones and vice-versa, over the same areas. In both cases (Figs 7b and 7c), the correlation is slightly higher over sea areas characterized by the presence of fine aerosols (e.g. Black Sea or Persian Gulf) and lower over seas undergoing frequent transport of coarse dust particles (e.g. southern Mediterranean Sea, Arabian Sea or Atlantic Ocean off the western African coasts). The overall computed correlation coefficient between g_{aer} and AE is equal to -0.95 over the Black Sea, -0.89 over the Mediterranean Sea, -0.87 and -0.94 over the Arabian Sea and Persian Gulf, respectively and -0.89 off the western African coasts (values given for $AE_{550-865}$ and g_{aer} data at 870 nm). These results indicate that the spatial patterns of MODIS C051 g_{aer} product are reasonable as compared to the C051 Ångström exponent data. This shows that the use of g_{aer} in modeling studies can be considered as reasonably reliable with regards to the consideration of fine and coarse aerosols over the examined study area, with slightly more confidence over areas characterized by the presence of fine particles, such as the Black Sea or Persian Gulf.

Since questions may also arise about possible uncertainties regarding the long-term variability of MODIS C051 aerosol size products, due to the calibration issues discussed in the previous section, the corresponding MODIS C006 AE product is displayed in Fig. 8a. Figs. 8a and 7a are similar in the main geographical patterns of the two collections' AE product. The similarity between C051 and C006 AE data is also depicted in the computed correlation coefficients (Fig. 8b), exceeding 0.8, and biases (in absolute and relative percentage terms, Figs 8c and 8d, respectively). For the Mediterranean Sea, the Arabian Sea and Persian Gulf, biases are smaller than 0.1 or 10% in most areas and 0.2 or 20% almost everywhere. Relative biases larger than 30% are only observed over the open Atlantic Ocean). The overall computed correlation coefficient for the entire study region is 0.88 (0.86, 0.89, 0.95 and 0.84 for Mediterranean, Arabian, Persian and Atlantic sea surfaces off the western African coasts). The corresponding overall relative percent bias is equal to 15.6% (9.1, 6.7, 6.1 and 15.7 for the same sub-areas as above). Our results indicate that the uncertainty related to the use of C051 AE data is small, especially over the Mediterranean Sea, the Arabian Sea, the Persian Gulf and the Atlantic Ocean areas not far from the European, African and Asian coastlines. Our AE results are in line with those of Levy et al.

(2013, Fig. 15) which refer, however, only to year 2008 (ours are for 2002-2010). In addition, a comparison is attempted in Figs 8e and 8f between the computed trends of C051 and C006 AE data over the common period 2002-2010, in order to assess whether changes are detected, which could be an indication of possible changes in corresponding asymmetry parameter trends. Figures 8e and 8f show the computed deseasonalized trends of slope values for both C051 and C006 AE. The results reveal similar patterns between C051 and C006. Small trends are found in both of them, in agreement with the small trends of asymmetry parameter reported in Fig. 5. We find that the sign of AE trends basically does not change from C051 to C006. This might be a signal that no changes of aerosol asymmetry parameter are expected in C006 and puts confidence on the C051 results given in the present study.

4 Evaluation against AERONET data

In this section we compare the satellite-measured aerosol asymmetry parameter with measurements from the global network of surface stations of AERONET, which is considered as the reference dataset (Holben et al., 1998). For this purpose, we identified the AERONET stations inside our area of interest and finally utilised only the coastal ones, so that both satellite and surface data be available. The total number of these stations is 69, and their locations are shown in Fig. 1 (open and full circles).

Table 1 contains the comparison statistical metrics for all wavelengths (Pearson correlation coefficient, bias, root mean square error (RMSE), slope, intercept) of the comparison between surface daily mean data from AERONET and satellite data from MODIS-Terra and MODIS-Aqua, which correspond to the 1°x1° cell wherein each station is located. For this analysis, we use all cells and days with common data between Terra-AERONET and Aqua-AERONET. The mean differences are calculated as g_{aer}(AERONET)-g_{aer}(Aqua) and g_{aer}(AERONET)-g_{aer}(Terra).

In general, we may note that on an annual level, the MODIS-Terra and Aqua asymmetry parameter values at 470 nm are not in very good agreement with the respective data from AERONET at 440 nm, while the results at the largest wavelengths are more reassuring, though not being very satisfactory (increasing R and decreasing relative bias and RMSE values at 675/660 nm and 870 nm). At 870 nm (Table 1 and Fig. 9), correlation coefficients are found to be the largest and equal to 0.47 (AERONET-Terra) and 0.46 (AERONET-Aqua), while satellite data are slightly overestimated compared to the surface data (bias -0.035 or 5.54% and -0.015 or -2.43%, respectively).

It is important to note that the agreement of satellite and surface data is better in spring and summer, for all studied wavelengths. Specifically, in case of MODIS-Aqua g_{aer}, the correlation coefficients increase up to 0.35, 0.50 and 0.54 at 440/470 nm, 660/675 nm and 870 nm, respectively, while the bias decreases down to 0.0005 (0.07%), 0.003 (0.46%) and 0.007 (1.11%), respectively.

Moreover, we find that for all seasons g_{aer} values at 870 nm and 660 nm, both from MODIS-Terra and MODIS-Aqua, are overestimated compared to $g_{aer\ (AERONET)}$ at the corresponding wavelengths (stronger overestimation at 870 nm and by Terra). Finally we note an underestimation of g_{aer} at 470 nm from MODIS-Aqua, relative to the data by AERONET at 440 nm, while very small biases (<0.5 %) are found between Terra and AERONET at the same wavelengths.

In Fig. 9 we present a scatterplot comparison between MODIS and AERONET g_{aer} data pairs. There is bias towards larger g_{aer} values from both Aqua and Terra compared to AERONET, with Terra overpredicting more than Aqua. The root mean square error to the fit between MODIS and AERONET is very similar between Aqua and Terra. There are concerns on the application of ordinary least squares regression, arising from the assumption that as the assigned independent variable, AERONET values should be free from error. We cannot guarantee the validity of this assumption, so we recognize that the reported R and slope values from Fig. 9 and Table 1, if viewed as metrics of agreement between MODIS g_{aer} and real g, may be subject to the effect of regression dilution and consequently biased low. This possible bias for R and slope could be neglected only if AERONET errors can also be considered negligible. With the above caveat in mind, the applied least-squares fit line to the scatterplot comparison between matched MODIS-AERONET data pairs (Fig. 9) indicates that MODIS overestimates g_{aer} more in the smaller than larger values, i.e. more for fine than coarse particles.

We present the frequency distributions of asymmetry parameter daily values (Fig. 10) on the days when data from all three databases (MODIS-Terra, MODIS-Aqua and AERONET) were provided. Fig. 10a corresponds to the whole area of interest, while Figs. 10b and c correspond to two broad sub-regions with basic differences in the aerosol source, namely Europe with great anthropogenic sources, and Africa, Middle East and Arabian peninsula, with predominant natural sources and mainly desert dust.

There is an apparent skew in the MODIS-Terra and MODIS-Aqua g_{aer} distributions, while the AERONET distributions are more symmetrical. Moreover, the satellite data distributions show larger values and smaller standard deviations compared to AERONET, with the Terra overestimation being more exaggerated. The disagreement is more pronounced in the sub-region of Europe, while in the sub-region of North Africa / Arabian peninsula, the distributions of satellite and surface data agree more thus confirming the finding of Fig. 9 based on the slope of applied linear regression fit. Values over Europe are generally smaller than over North Africa / Arabian peninsula (Fig. 3), which can be attributed to the presence of larger size particles of desert origin in the latter sub-region, in contrast to Europe, where due to industrial activity and frequent biomass burning the presence of smaller size particles is important. Therefore, the smaller g_{aer} values (<0.6) in the frequency distributions of the whole area, are overwhelmingly contributed by the European sub-region, contrasting with larger values (0.7-0.75) being contributed by both sub-regions and even more by N. Africa/Arabian peninsula at larger g_{aer}.

The overall comparison between satellite and surface g_{aer} data performed in the scatterplot of Fig. 9 and Table 1 does not allow one to have an insight to how the comparison behaves spatially, namely how it differs from one region to another. This is addressed in Fig. 11, showing the comparison of satellite and surface data at the wavelength of 870 nm separately between MODIS-Terra - AERONET and MODIS-Aqua – AERONET. For this comparison, we selected AERONET stations for which there is satisfactory overlap between the time series from AERONET and the time series from MODIS, namely the number of common days between AERONET-Terra and AERONET-Aqua is larger than 100. This criterion is satisfied by 36 stations for AERONET-Terra and by 34 for AERONET-Aqua shown in Fig. 11. For each AERONET station we compute the Pearson correlation coefficient between the station data and the corresponding MODIS-Terra or Aqua data at 870 nm, for the 1°x1° cell containing the station. Moreover, there is the information if the trends between AERONET and either MODIS-Terra or Aqua have the same sign (blue color) or not (red color).

In the case of the $g_{aer\ (AERONET)} - g_{aer\ (Terra)}$ comparison, at 5 stations, (i.e. in 14% of total 36 stations), the correlation coefficient R is larger than 0.5 (largest R found is 0.64 at station “Bahrain”), while at 13 stations (36 %) and 26 stations (72%) R is larger than 0.4 and 0.3, respectively.. With respect to the agreement on the sign of the trends, at 24 out of 36 stations (67%) there is a trend sign match and at 12 stations (33%) a mismatch. Nevertheless, it should be noted that no systematic spatial behaviour, i.e. homogeneous spatial patterns, is found concerning the performance of MODIS-Terra g_{aer} against AERONET in terms of either the magnitude of correlation or the agreement of trends between the satellite and ground datasets. A similar picture emerges for the comparison $g_{aer\ (AERONET)}$ – $g_{aer\ (Aqua)}$. In this case, there are again 5 stations (15% of total 34 stations) with R>0.5 (maximum value R=0.61 again at "Bahrain"), while at 13 stations (38%) and24 stations (71%) R is larger than 0.4 and 0.3, respectively. Also, we see that at 22 stations (65%) there is a trend sign match and at 12 (35%) there is a mismatch.

5 Summary and Conclusions

Using satellite data from collection (051) of MODIS-Terra and Aqua data, we examine the spatiotemporal variations of the aerosol asymmetry parameter (g_{aer}) over North Africa, the Arabian peninsula and Europe. To our knowledge, this is the first time that a satellite (MODIS) based dataset of g_{aer}, assessed and evaluated (against AERONET data), is used for the study region. This is important, since such an evaluated satellite dataset is very useful for many applications, like radiative transfer and climate modelling as well as for remote sensing. The advantages of MODIS g_{aer} data are that:

(i) They ensure complete spatial coverage over sea surfaces surrounding Europe, Mediterranean and Middle East, which is essential for investigating and understanding physical processes related to aerosols. These processes are strongly dependent on the aerosol radiative and optical properties, g_{aer} being one of the three key ones (the other two being aerosol optical thickness and single scattering albedo). Such a complete spatial coverage is especially required by radiative transfer and climate models.

(ii) They provide with spectral g_{aer} values, at 7 wavelengths from 470 to 2130 nm, which are of essential importance for radiative transfer models. Such spectrally resolved aerosol optical properties can induce significant differences in model computations of aerosol radiative effects (Hatzianastassiou et al., 2007).

(iii) They provide a relatively long temporal coverage, i.e. 8 years, which is significant for examining seasonal and inter-annual cycles and changes of this aerosol optical property, especially combined with the complete spatial coverage. This is also important since it provides a reasonable statistical bed for attempting evaluations through comparison against other g_{aer} data like the AERONET.

(iv) They constitute the first to know so far satellite based g_{aer} dataset; until now, the utilized g_{aer} data in modelling or other analyses were taken from in-situ measurements or aerosol models, which both have their own deficiencies, namely limited spatial coverage or pure theoretical basis.

According to the obtained results, generally, the largest values of the asymmetry parameter, indicating the strongest forward scattering of radiation by atmospheric aerosols, are found over areas with aerosol load being dominated by large size particles of desert dust (tropical Atlantic, Arabian and Red Seas),. On the contrary, smaller g_{aer} values are seen where a significant fraction of aerosol load comes from small size particles of anthropogenic origin, e.g. over the Black Sea. The results are consistent with the theory and thus prove a good performance of the MODIS retrieval of aerosol asymmetry parameter. Depending on the area of interest, the seasonal cycle of the asymmetry parameter varies markedly. More specifically, in areas with abundance of desert dust particles, the range of intra-annual variation is small, with the largest values during summer, while in other areas the seasonality is reversed, with the largest values during the cold season and the smallest during the warm season. The asymmetry parameter decreases with wavelength, especially when one examines its spatially minimum values, while this decrease is weaker for the larger g_{aer} values, corresponding to the presence of coarser particles.

The seasonal fluctuation is more pronounced with increasing wavelength in the examined regions, which is attributed to the different spectral behaviour of the asymmetry parameter for small and large particles. With respect to the inter-annual variability of the asymmetry parameter, we did not discern very important either increasing or decreasing tendencies, with absolute changes smaller than 0.04 in any case. On the other hand, we found opposing tendencies for the two satellite datasets. MODIS-Terra observes mostly increasing tendencies, while Aqua gives also a few regions with decreasing tendencies. Generally, the largest intra-annual and inter-annual variations are seen over the Black Sea, while the smallest over the tropical Atlantic. However, some strong trends (especially from Terra) may be due to calibration drift errors, which may be addressed in collection 006. Along these lines we performed some preliminary comparisons between 051 and 006 Ångström Exponent trends from Aqua, which ensured that AE and g_{aer} are very closely anti-correlated. These preliminary results, show that 051 Aqua AE trends resemble very closely the 006 trends, supporting that the g_{aer} trends from collection 051 (at least for Aqua) reported in this study are credible.

The 051 MODIS g_{aer} data is not a retrieved but a derived MODIS parameter. Given that the retrieval is strongly dependent on the assumptions made, namely on the aerosol modes used, uncertainties can be associated with its use in radiative transfer modeling. In order to examine these uncertainties, the g_{aer} data were compared with 051 AE data for the same period. The results from the comparison showed a strong anti-correlation (coefficient higher than 0.7-0.8) proving the consistency and reasonably safe use of g_{aer} data in modeling studies, at least to the same degree with MODIS AE data in modeling and other analyses. The correlation is even higher over sea areas characterized by stronger presence of fine aerosols, like the Black Sea, the Persian Gulf or the North Sea. This confidence is further strengthened by the small identified uncertainties related with the use of collection 051 instead of 006 MODIS g_{aer} data reported in the previous paragraph. This was obtained indirectly based on the use of AE data of both collections since g_{aer} data are not yet available in collection 006.

We compare satellite data with surface data from the AERONET, in order to further validate the reliability of the former. Through the examination of frequency distributions of daily g_{aer}, a shift of satellite data towards larger values relative to surface data becomes apparent. This finding is more pronounced for g_{aer} over Europe, while the North African, Arabian peninsula values are more in agreement. Moreover, the smallest g_{aer} values originate from particles from Europe, because of the generation of smaller size particles by industrial activities and biomass burning.

We present scatter plots of daily g_{aer} values between MODIS-Terra, MODIS-Aqua, and AERONET, which show moderate agreement between satellite data at 470 nm and surface data at 440 nm, with small correlation coefficients ($R<0.3$) and a slight underestimation by MODIS. Slightly better agreement was noted at larger wavelengths, but still without reaching very satisfactory levels ($R<0.47$). Nevertheless, during spring and summer, satellite and surface measurements tend to agree more. Finally, for the comparisons at 660/675 and 870 nm, we report an overestimation of g_{aer} by MODIS compared to AERONET,.

When examined at the local scale, i.e. station by station, the MODIS g_{aer} data agree reasonably and for some stations better than in overall, but still not very well, with those of AERONET. This analysis, based on 36 and 34 AERONET stations ensuring at least 100 common days with MODIS-Terra and Aqua, respectively, shows that in 36 and 38% of stations, respectively, the MODIS data have correlation coefficients larger than 0.4 (reaching values up to 0.64), while in about 65% of stations the trends of g_{aer} from MODIS and AERONET have the same sign. Nevertheless, the magnitude of correlation coefficients or the agreement between trends of g_{aer} from the satellite and ground datasets do not exhibit a systematic (homogeneous) spatial pattern.

Our results offer an interesting way to assess the uncertainty induced by the use of such satellite g_{aer} data in climate and radiative transfer models that compute aerosol radiative and climate effects. Based on an overall assessment of satellite MODIS g_{aer} through detailed comparisons against ground AERONET data, it appears that in overall MODIS performs satisfactorily in terms of magnitude of g_{aer} values. This is indicated by the computed biases, which are smaller than 5% with respect to MODIS values, with better performance at smaller wavelengths. The root mean squared errors vary within the range 5-10% again being smaller for smaller wavelengths.These results indicate an uncertainty of MODIS g_{aer} data over the study region up to of 10% at maximum. Previous analyses and sensitivity studies for the same study region (Papadimas et al., 2012) have shown that such g_{aer} uncertainties can induce modifications of aerosol direct radiative effects (DREs) which are equal to 30% at the top-of-atmosphere (TOA) and 1% in the atmosphere and 10% at the surface, at maximum. Therefore, the uncertainty associated with the use of MODIS g_{aer} is larger as to any aerosol related physical process taking place at TOA, namely planetary cooling or warming and its magnitude, smaller for processes at the Earth's surface, e.g. surface cooling and very small for aerosol processes and feedbacks in the atmosphere, like the aerosol semi-direct effect and its implications. Results from the same previous analysis (Papadimas et al., 2012) proved that the exact magnitude of MODIS g_{aer} DRE uncertainty can be estimated by simple linear equations relating DREs and g_{aer}, separately given for TOA, atmosphere and surface.

The results of the present analysis are useful since they assess for the first time the performance of satellite based products of aerosol asymmetry parameter over broad regions of special climatic interest. The obtained results are relatively satisfactory given the difficulties encountered by satellite retrieval algorithms due to the different assumptions they made. Nevertheless, our results and identified weaknesses remind that users should be aware of the g_{aer} uncertainties and their consequences. The identified weaknesses may provide an opportunity to improve such satellite retrievals of aerosol asymmetry parameter in forthcoming data products like those of MODIS C006. The increased temporal coverage of g_{aer} data, combined with the continued operation of MODIS, is expected to make possible the building of the first real satellite climatology of this important aerosol optical property.

6 Acknowledgments

This research has been co-financed by the European Union (European Social Fund – ESF) and Greek national funds through the operational programme “Education and Lifelong Learning” of the National Strategic ReferenceFramework (NSRF) – Research Funding Program: THALES. Investing in knowledge society through the European Social Fund. The Collection 051 MODIS-Terra data were obtained from NASA’s Level 1 and Atmosphere Archive and Distribution System (LAADS) website (ftp://ladsweb.nascom.nasa.gov/). We would like to thank the principal investigators maintaining the AERONET sites used in the present work.

References

Alonso-Pérez S., Cuevas E., Querol X., Guerra J. C., and Pérez C. (2012). African dust source regions for observed dust outbreaks over the Subtropical Eastern North Atlantic region, above 25°N, J. Arid Environ., 79, 100-109, doi:10.1016/j.jaridenv.2011.11.013.

Barnaba F. and G. P. Gobbi: Aerosol seasonal variability over the Mediterranean region and relative impact of maritime, continental and Saharan dust particles over the basin from MODIS data in the year 2001, Atmospheric Chemistry and Physics, 4, 4285 - 4337, SRef-ID: 1680-7375/acpd/2004-4-4285SRef-ID: 1680-7375/acpd/2004-4-4285, 2004.

Barnaba F., Angelini F., Curci G., and Gobbi G. P. (2011), An important fingerprint of wildfires on the European aerosol load, Atmos. Chem. Phys., 11, 10,487–10,501.

Bovchaliuk A., Milinevsky G., Danylevsky V., Goloub P., Dubovik O., Holdak A., and Sosonkin, M. (2013). Variability of aerosol properties over Eastern Europe observed from ground and satellites in the period from 2003 to 2011. Atmos. Chem. Phys., 13, 6587-6602

Bréon F.-M., Vermeulen A., and Descloitres J. (2011). An evaluation of satellite aerosol products against sunphotometers measurements, Remote Sens. Environ., 115, 3102–3111.

Chubarova, N. Y.: Seasonal distribution of aerosol properties over Europe and their impact on UV irradiance, Atmos. Meas. Tech., 2, 593–608, doi:10.5194/amt-2-593-2009, 2009.

Di Iorio, T., A. di Sarra, W. Junkermann, M. Cacciani, G. Fiocco, and D. Fua, Tropospheric aerosols in the Mediterranean: 1. Microphysical and optical properties, J. Geophys. Res., 108(D10), 4316, doi:10.1029/2002JD002815, 2003

Dubovik, Oleg, Brent Holben, Thomas F. Eck, Alexander Smirnov, Yoram J. Kaufman, Michael D. King, Didier Tanré, Ilya Slutsker, 2002: Variability of Absorption and Optical Properties of Key Aerosol Types Observed in Worldwide Locations. *J. Atmos. Sci.*, **59**, 590–608.

Dubovik, O. and M. D. King, 2000: A flexible inversion algorithm for retrieval of aerosol optical properties from Sun and sky radiance measurements," J. Geophys. Res., 105, 20 673-20 696.

Engelstaedter S., Tegen I., and Washington R. (2006). North African dust emissions and transport, Earth-Sci. Revi., 79(1-2), 73-100.

Fotiadi, A., E. Drakakis, N. Hatzianastassiou, C. Matsoukas, K. G. Pavlakis, D. Hatzidimitriou, E. Gerasopoulos, N. Mihalopoulos, and I. Vardavas (2006), Aerosol physical and optical properties in the eastern Mediterranean Basin, Crete, from Aerosol Robotic Network data, Atmos. Chem. Phys., 6, 5399– 5413.

Gerasopoulos, E., Kouvarakis, G., Babasakalis, P., Vrekoussis, M., Putaud, J. P., and Mihalopoulos, N.: Origin and variability of particulate matter (PM10) mass concentrations over the Eastern Mediterranean, Atmos. Environ., 40, 4679–4690, 2006.

Ginoux P, Prospero J. M., Gill T. E., Hsu C. N., Zhao M., (2012). Global-scale attribution of anthropogenic and natural dust sources and their emission rates based on MODIS Deep Blue aerosol products. Rev. Geophys. 50, RG3005. doi:10.1029/2012RG000388.

Gkikas, A., Hatzianastassiou, N., and Mihalopoulos, N.: Study and characterization of aerosol episodes in the Mediterranean basin for the 7-year period 2000–2007 based on MODIS data, European Aerosol Conference, Greece, Thessaloniki, 24–29 August 2008.

Gkikas, A., Hatzianastassiou, N., and Mihalopoulos, N.: Aerosol events in the broader Mediterranean basin based on 7-year (2000–2007) MODIS C005 data, Ann. Geophys., 27, 3509–3522, doi:10.5194/angeo-27-3509-2009, 2009.

Gkikas, A., Houssos, E., Hatzianastassiou, N., Papadimas, C. and Bartzokas, A. (2011), Synoptic conditions favouring the occurrence of aerosol episodes over the broader Mediterranean basin. Q.J.R. Meteorol. Soc.. doi: 10.1002/qj.978.

Gkikas, A., Hatzianastassiou, N., Mihalopoulos, N., Katsoulis, V., Kazadzis, S., Pey, J., and Torres, O. (2013). The regime of intense desert dust episodes in the Mediterranean based on contemporary satellite observations and ground measurements. Atmos. Chem. Phys., 13, 12135-12154.

Gkikas A., Houssos E. E., Lolis C. J., Bartzokas A., Mihalopoulos N., and Hatzianastassiou N. (2014), Atmospheric circulation evolution related to desert-dust episodes over the Mediterranean. Quart. J. Roy. Meteorol. Soc., 690, 1634-1645.

Goloub, P., and O. Arino, 2000: Verification of the consistency of POLDER aerosol index over land with ATSR-2 fire product. Geophys. Res. Lett., 27, 899–902.

Graßl, H.: Possible changes of planetary albedo due to aerosol particles, in Man’s Impact on Climate, edited by: W. Bach, J. Pankrath, and W. Kellogg, Elsevier, New York, 1979.

Hansen, J., Sato, M., and Ruedy, R.: Radiative forcing and climate response, J. Geophys. Res., 102, 6831–6864, 1997.

Hatzianastassiou, N., B. Katsoulis, I. Vardavas: Sensitivity analysis of aerosol direct radiative forcing in ultraviolet - visible wavelengths and consequences for the heat budget, Tellus, 56b, 368 - 381, 2004.

Hatzianastassiou, N., A. Gkikas, N. Mihalopoulos, O. Torres, and B. D. Katsoulis: Natural versus anthropogenic aerosols in the eastern Mediterranean basin derived from multiyear TOMS and MODIS satellite data, J. Geophys. Res., 114, D24202, doi:10.1029/2009JD011982, 2009.

Hatzianastassiou, N., Matsoukas, C., Drakakis, E., Stackhouse Jr., P. W., Koepke, P., Fotiadi, A., Pavlakis, K. G., and Vardavas, I.: The direct effect of aerosols on solar radiation based on satellite observations, reanalysis datasets, and spectral aerosol optical properties from Global Aerosol Data Set (GADS), Atmos. Chem. Phys., 7, 2585-2599, doi:10.5194/acp-7-2585-2007, 2007.

Haywood, J.M., and O. Boucher, 2000: Estimates of the direct and indirect radiative forcing due to tropospheric aerosols: A review.Rev. Geophys., 38, 513–543.

Heishman, J. (1999), Commanding Officer, Forecaster's Handbook, U.S. Navy Cent. Meteorol. and Oceanogr. Cent., Manama, Bahrain.

Holben B.N., T.F. Eck, I. Slutsker, D. Tanré, J.P. Buis, A. Setzer, E. Vermote, J.A. Reagan, Y. Kaufman, T. Nakajima, F. Lavenu, I. Jankowiak, and A. Smirnov, 1998: AERONET - A federated instrument network and data archive for aerosol characterization, Rem. Sens. Environ., 66, 1-16.

Ichoku C., D. Allen Chu,ShanaMattoo,Yoram J. Kaufman, Lorraine A. Remer, Didier Tanre´, IlyaSlutsker, and Brent N. Holben: A spatio-temporal approach for global validation and analysis of MODIS aerosol products. GEOPHYSICAL RESEARCH LETTERS, VOL. 29, NO. 12, 10.1029/2001GL013206, 2002.

IPCC, 2007: Climate Change 2007: The Physical Science Basis. Contribution of Working Group I to the Fourth Assessment Report of the Intergovernmental Panel on Climate Change [Solomon, S., D. Qin, M. Manning, Z. Chen, M. Marquis, K.B. Averyt, M.Tignor and H.L. Miller (eds.)]. Cambridge University Press, Cambridge, United Kingdom and New York, NY, USA.

IPCC, 2013: Climate Change 2013: The Physical Science Basis. Contribution of Working Group I to the Fifth Assessment Report of the Intergovernmental Panel on Climate Change [Stocker, T.F., D. Qin, G.-K. Plattner, M. Tignor, S.K. Allen, J. Boschung, A. Nauels, Y. Xia, V. Bex and P.M. Midgley (eds.)]. Cambridge University Press, Cambridge, United Kingdom and New York, NY, USA, 1535 pp.

Joseph J. H., Wiscombe W. J., and Weinman, J. A. (1976). The delta-Eddington approximation for radiative flux transfer. J. Atmos. Sci., 33, 2452–2459.

Jianrong Bi, Jianping Huang, Qiang Fu, XinWanga, Jinsen Shi , Wu Zhang , Zhongwei Huang, Beidou Zhang: Toward characterization of the aerosol optical properties over Loess Plateau of Northwestern China. Journal of Quantitative Spectroscopy &Radiative Transfer 112 (2011) 346–360.

Kalapureddy, M. C. R., D. G. Kaskaoutis, P. Ernest Raj, P. C. S. Devara, H. D. Kambezidis, P. G. Kosmopoulos, and P. T. Nastos (2009), Identification of aerosol type over the Arabian Sea in the premonsoon season during the Integrated Campaign for Aerosols, Gases and Radiation Budget (ICARB), J. Geophys. Res., 114, D17203, doi:10.1029/2009JD011826.

Kalivitis, N., Gerasopoulos, E., Vrekoussis, M., Kouvarakis, G., Kubilay, N., Hatzianastassiou, N., Vardavas, I., and Mihalopoulos, N.: Dust transport over the eastern Mediterranean derived from TOMS, AERONET and surface measurements, J. Geophys. Res., 112, D03202, doi:10.1029/2006JD007510, 2007.

Kaufman, Y. J., D. Tanré, L. A. Remer, E. F. Vermote, A. Chu, and B. N. Holben: Operational remote sensing of tropospheric aerosol over land from EOS moderate resolution imaging spectroradiometer, J. Geophys. Res., 102, 17,051– 17,067, 1997.

Kinne, S., D. O'Donnel, P. Stier, S. Kloster, K. Zhang, H. Schmidt, S. Rast, M. Giorgetta, T. F. Eck, and B. Stevens (2013), MAC-v1: A new global aerosol climatology for climate studies, J. Adv. Model. Earth Syst., 5, 704–740, doi:10.1002/jame.20035.

Kishcha, P., A. M. da Silva, B. Starobinets, C. N. Long, O. Kalashnikova, and P. Alpert, Meridional distribution of aerosol optical thickness over the tropical Atlantic Ocean, Atmos. Chem. Phys. Discuss., 14, 23309-23339, 2014.

Koepke, P., M. Hess, I.Schult, and E. P. Shettle: Global aerosol data set, Rep. No. 243, Max-Planck InstitutfuerMeteorologie, Hamburg, Germany, 44 pp., 1997.

Kondratyev, K. Y. 1999. Climatic effects of aerosols and clouds. Springer, New York.

Kutiel H., Furman, H., (2003). Dust storms in the Middle East: sources of origin and their temporal characteristics. Indoor Built Environ. 12, 419–426.

Lelieveld, J., et al. (2002), Global air pollution crossroads over the Mediterranean, Science, 298, 794– 799, doi:10.1126/science.1075457.

Levy, R. C., Remer, L. A., Kleidman, R. G., Mattoo, S., Ichoku, C., Kahn, R., and Eck, T. F.: Global evaluation of the Collection 5 MODIS dark-target aerosol products over land, Atmos. Chem. Phys., 10, 10399-10420, doi:10.5194/acp-10-10399-2010, 2010.

Lohmann U., Feichter, J. [2005] Global indirect aerosol effects: A review . Atmos. Chem. Phys., 5, 715-737.

Miller S. D., Kuciauskas A. P., Liu M., Ji Q., Reid J. S., Breed D. W. Walker A. L., and Mandoos A. A.. (2008). Haboob dust storms of the southern Arabian Peninsula, J. Geophys. Res., 113, *D01202, doi:*10.1029/2007JD008550.

Nabat P., Somot S., Malle, M., Chiapello I., Morcrette J. J., Solmon F., Szopa S., Dulac F., Collins W., Ghan S., Horowitz L. W., Lamarque J. F., Lee Y. H., Naik V., Nagashima T., Shindell D., and Skeie R. (2013), A 4-D climatology (1979–2009) of the monthly tropospheric aerosol optical depth distribution over the Mediterranean region from a comparative evaluation and blending of remote sensing and model products. Atmos. Meas. Tech., 6, 1287–1314.

Lyamani, H., F. J. Olmo, A. Alca´ntara, and L. Alados-Arboledas (2006), Atmospheric aerosols during the 2003 heat wave in southeastern Spain. I: Spectral optical depth, Atmos. Environ., 40, 6453 – 6464, doi:10.1016/ j.atmosenv.2006.04.048.

Papadimas, C. D., N. Hatzianastassiou, N. Mihalopoulos, X. Querol, and I. Vardavas (2008), Spatial and temporal variability in aerosol properties over the Mediterranean basin based on 6-year (2000–2006) MODIS data, J. Geophys. Res., 113, D11205, doi:10.1029/2007JD009189.

Papadimas C. D., Hatzianastassiou N., Matsoukas C., Kanakidou M., Mihalopoulos N., and Vardavas, I. (2012). The direct effect of aerosols on solar radiation over the broader Mediterranean basin. Atmos. Chem. Phys., 12, 7165-7185.

Pace, G., A. di Sarra, Meloni, D., Piacentino, S., and Chamard, P.: Aerosol optical properties at Lampedusa (Central Mediterranean). 1. Influence of transport and identification of different aerosol types, Atmos. Chem. Phys., 6, 697–713, 2006, www.atmos-chem-phys.net/6/697/2006/.

Pandithurai, R. T. Pinker, P. C. S. Devara, T. Takamura, K. K. Dani, Seasonal asymmetry in diurnal variation of aerosol optical characteristics over Pune, western India, J. Geophys. Res., 112, D8, DOI: 10.1029/2006JD007803, 2007.

Pilinis, Ch., Pandis, S. N. and Seinfeld, J. H. 1996. Sensitivity of direct climate forcing by anthropogenic aerosols to aerosol size distribution and composition. J. Geophys. Res. 100, 18 739–18 754.

Prospero, J., P. Ginoux, O. Torres, and S. E. Nicholson (2002), Environmental Characterization of Global sources of atmospheric soil dust derived from the NIMBUS-7 TOMS absorbing aerosol product, Rev. Geophys., 40(1), 1002, doi:10.1029/20000GR000095.

Rahul, PRC and Salvekar, PS and Devara, PCS (2008) Aerosol optical depth variability over Arabian Sea during drought and normal years of Indian monsoon. Geophysical Research Letters, 35 (22).

Rashki A., Kaskaoutis D. G., de W. Rautenbach C. J., Eriksson P. G., Qiang M, and Gupta P., (2012). Dust storms and their horizontal dust loading in the Sistan region, Iran. Aeolian Res 5: 51–62.

Rashki A., Kaskaoutis D. G., Eriksson P. G., de W. Rautenbach C. J., Flamant C., Abdi Vishkaee F., (2014). Spatio-temporal variability of dust aerosols over the Sistan region in Iran based on satellite observations. Nat. Hazards, doi: 10.1007/s11069-013-0927-0.

Remer L.A., Tanre D., Kaufman Y.J., Levy R, and Matoo S.: Algorithm for Remote Sensing of Tropospheric Aerosol from MODIS: Collection 005, 2006, http://modis.gsfc.nasa.gov/data/atbd/atbd_mod02.pdf.

Remer L.A., Kaufman Y.J., Tanre D. and co-authors: The MODIS aerosol algorithm, products, and validation, J. Atmos. Sci., 62: 947-973, 2005.

Remer LA, Kleidman RG, Levy RC, Kaufman YJ, Tanr'e D, Mattoo S, Martins JV, Ichoku C, Koren I, Yu H, Holben BN. 2008. Global aerosol climatology from the MODIS satellite sensors. Journal of Geophysical Research 113: D14S07, DOI: 10.1029/2007JD009661.

Satheesh, S. K., V. Ramanathan, X. Li-Jones, J. M. Lobert, I. A. Podgorny, J. M. Prospero, B. N. Holben, and N. G. Loeb, A model for the natural and anthropogenic aerosols over the tropical Indian Ocean derived from Indian Ocean Experiment data, J. Geophys. Res., 104, 27,421–27,440, 1999.

Satheesh, S. K., K. Krishna Moorthy, Y. J. Kaufman, and T. Takemura, Aerosol optical depth, physical properties and radiative forcing over the Arabian Sea, Meteorology and Atmospheric Physics, Volume 91, Issue 1, pp 45-62, 2006.

Savoie, D. L., J. M. Prospero, and R. T. Nees, Nitrate, nonsea-salt sulfate, and mineral aerosolover the northwestern Indian Ocean, J. Geophys. Res., 92, 933–942, 1987.

Sciare, J., H. Bardouki, C. Moulin, and N. Mihalopoulos (2003), Aerosol sources and their contribution to the chemical composition of aerosols in the Eastern Mediterranean Sea during summertime, Atmos. Chem. Phys., 3, 291–302, SRef-ID:1680 – 7324/acp/2003–3-291.

Smirnov A., Holben B. N., Dubovik O., O'Neill N. T., Eck T. F., Westphal D. L., Goroch A. K., Pietras C., and Slutsker I, 2002a: Atmospheric Aerosol Optical Properties in the Persian Gulf. *J. Atmos. Sci.*, **59**, 620–634, doi: http://dx.doi.org/10.1175/1520-0469(2002)059<0620:AAOPIT>2.0.CO;2.

Smirnov, A., B. N. Holben, Y. J. Kaufman, O. Dubovik, T. F. Eck, I. Slutsker, C. Pietras, and R. N. Halthore, 2002b: Optical properties of atmospheric aerosol in maritime environments. *J. Atmos. Sci.*, **59,** 501–523.

Smirnov, A., B. N. Holben, T. F. Eck, I. Slutsker, B. Chatenet, and R. T. Pinker, 2002c: Diurnal variability of aerosol optical depth observed at AERONET (Aerosol Robotic Network) sites, *Geophys. Res. Lett.*, **29,** 23, 2115, doi:10.1029/2002GL016305.

Tanré, D., Y. J. Kaufman, M. Herman, and S. Mattoo: Remote sensing of aerosol properties over oceans using the MODIS/EOS spectral radiances, J. Geophys. Res., 102, 16,971–16,988, 1997.

Tindale, N. W., and P. P. Pease, Aerosols over the Arabian Sea: Atmospheric transport pathways and concentrations of dust and sea salt, Deep Sea Res., 46, 1577–1595, 1999.

Yu, H., Dickinson, R. E., Chin, M., Kaufman, Y. J., Holben, B. N. Geogdzhayev, I. V., and Mishchenko, M. I.: Annual cycle of global distributions of aerosol optical depth from integration of MODIS retrievals and GOCART model simulations, J. Geophys. Res., 108, 4128, doi:10.1029/2002JD002717, 2003.

Zdun, A., A. Rozwadowska and S. Kratzer, 2011. Seasonal variability in the optical properties of Baltic aerosols, Oceanologia, 53(1), 7-34.

Zuluaga, M. D., P. J. Webster, and C. D. Hoyos (2012), Variability of aerosols in the tropical Atlantic Ocean relative to African Easterly Waves and their relationship with atmospheric and oceanic environments,J. Geophys. Res.,117, D16207, doi:10.1029/2011JD017181.

Table 1. Correlation coefficients (R), mean bias, root mean squared error (RMSE) and the slope and intercept values of applied linear regression fits between MODIS and AERONET g_{aer} data. The statistical parameters are given separately for the pairs of wavelengths: (i) 470 nm (MODIS) and 440 nm (AERONET), (ii) 660 nm (MODIS) and 675nm (AERONET) and (iii) 870 nm (MODIS and AERONET). The statistical parameters are also given separately for winter, spring, summer and autumn. [a]

MODIS-Terra

		R	Bias*	RMSE	Slope	Intercept
year	470-440	0.25	$2x10^{-4}$	0.045	0.36	0.45
	660-675	0.41	-0.028	0.060	0.55	0.32
	870	0.47	-0.035	0.070	0.60	0.29
Winter	470-440	0.20	$4.5x10^{-4}$	0.046	0.26	0.53
	660-675	0.35	-0.033	0.056	0.41	0.42
	870	0.41	-0.053	0.057	0.40	0.43
Spring	470-440	0.27	$-5x10^{-4}$	0.046	0.40	0.43
	660-675	0.44	-0.023	0.060	0.63	0.27
	870	0.50	-0.026	0.071	0.67	0.24
Summe	470-440	0.33	-0.002	0.044	0.51	0.35
	660-675	0.48	-0.031	0.061	0.71	0.22
	870	0.54	-0.030	0.077	0.79	0.16
Autumn	470-440	0.21	0.003	0.044	0.30	0.50
	660-675	0.33	-0.027	0.059	0.45	0.38
	870	0.41	-0.035	0.068	0.53	0.34

MODIS-Aqua

		R	Bias*	RMSE	Slope	Intercept
	470-440	0.27	0.018	0.047	0.41	0.40
	660-675	0.42	-0.005	0.062	0.61	0.26
	870	0.46	-0.015	0.072	0.61	0.26
W						

[a]The reported correlation coefficients and slopes may be biased low, because we did not include in our analysis the unknown AERONET errors.

inter	470-440	0.25	0.024	0.049	0.36	0.43
	660-675	0.39	-0.001	0.062	0.55	0.30
	870	0.43	-0.021	0.068	0.51	0.33
Spring	470-440	0.29	0.015	0.048	0.45	0.38
	660-675	0.45	-0.003	0.064	0.70	0.20
	870	0.50	-0.007	0.076	0.71	0.19
Summe	470-440	0.35	0.014	0.045	0.55	0.30
	660-675	0.50	-0.012	0.060	0.72	0.19
	870	0.53	-0.018	0.074	0.73	0.19
Autumn	470-440	0.20	0.021	0.047	0.30	0.47
	660-675	0.32	-0.003	0.061	0.46	0.36
	870	0.37	-0.014	0.069	0.48	0.34

* $g_{aer(AERONET)}$-$g_{aer(MODIS)}$

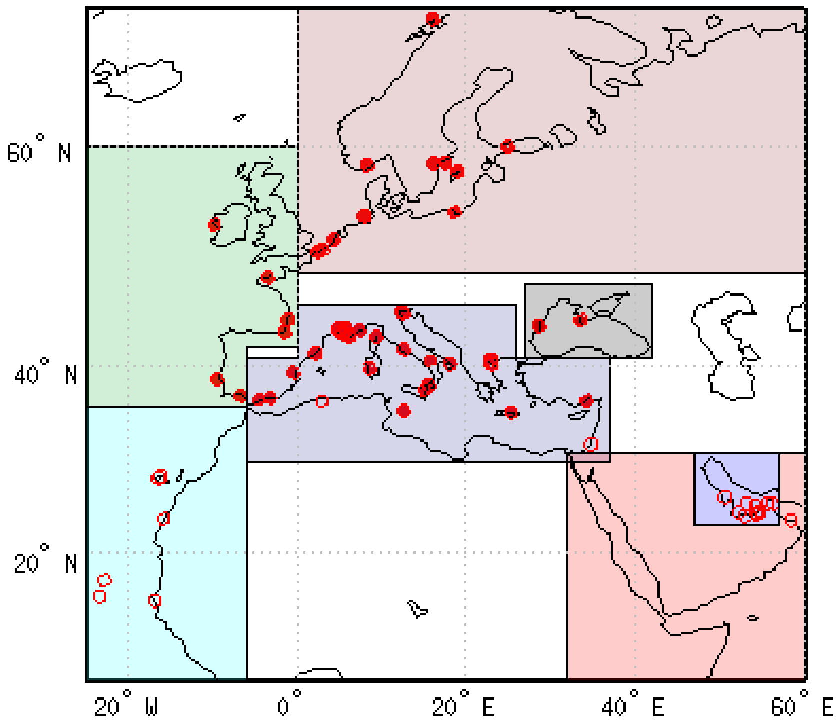

Figure 1. The study region (5°N–70°N, 25°W–60°E) and the location of 69 AERONET stations used for validation of MODIS satellite aerosol asymmetry parameter (g_{aer}) data. Solid red circles denote stations located in Europe and hollow red circles are stations in Africa, Middle East and the Arabian peninsula. Also shown are seven sub-regions selected for studying the seasonal variation of g_{aer}.

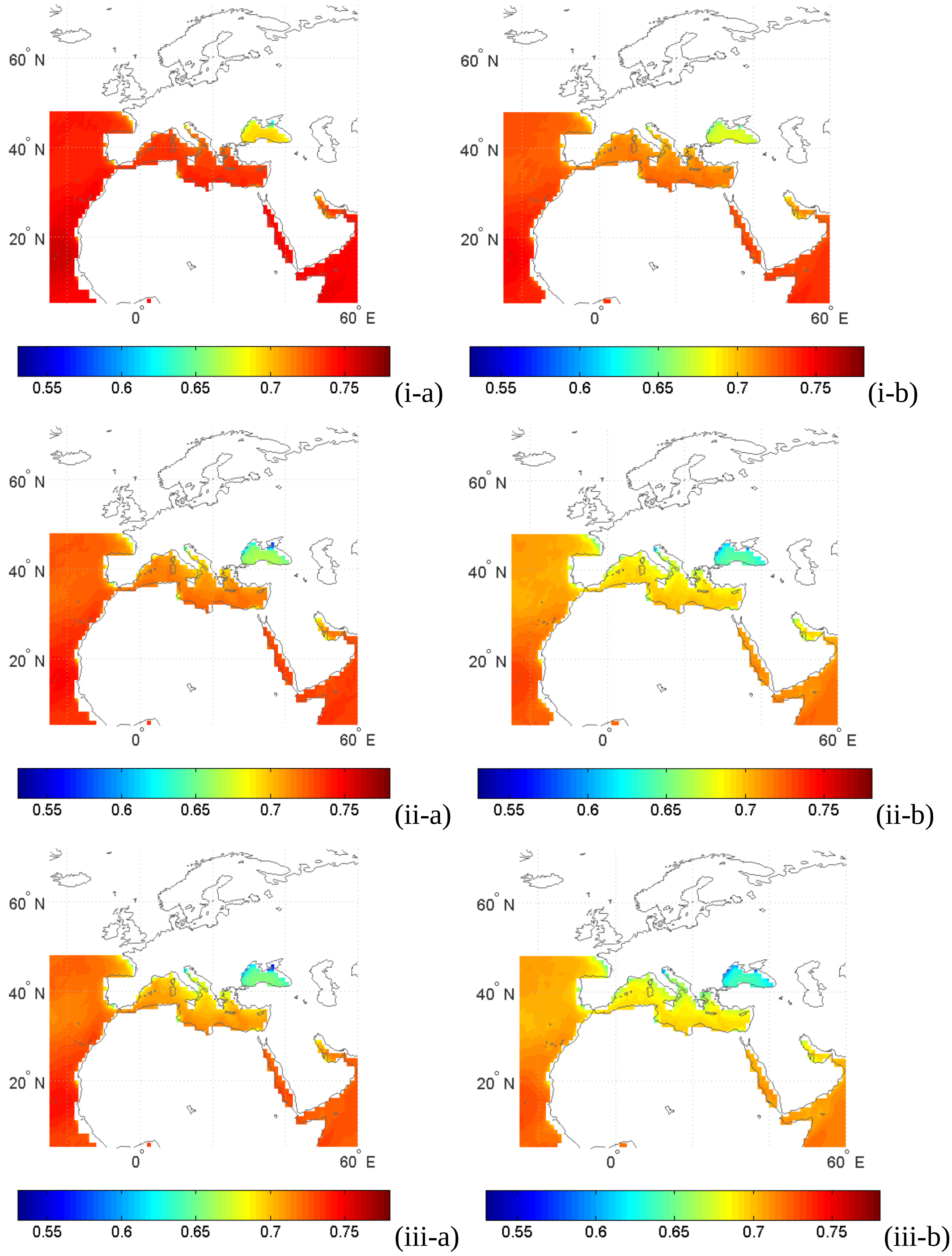

Figure 2. Geographical distribution of MODIS-Terra (-a, left column) and MODIS-Aqua (-b, right column) g_{aer} values averaged over 2002-2010, at the wavelengths of: 470 nm (i-, top row), 660 nm (ii-, middle row) and 870 nm (iii-, bottom row).

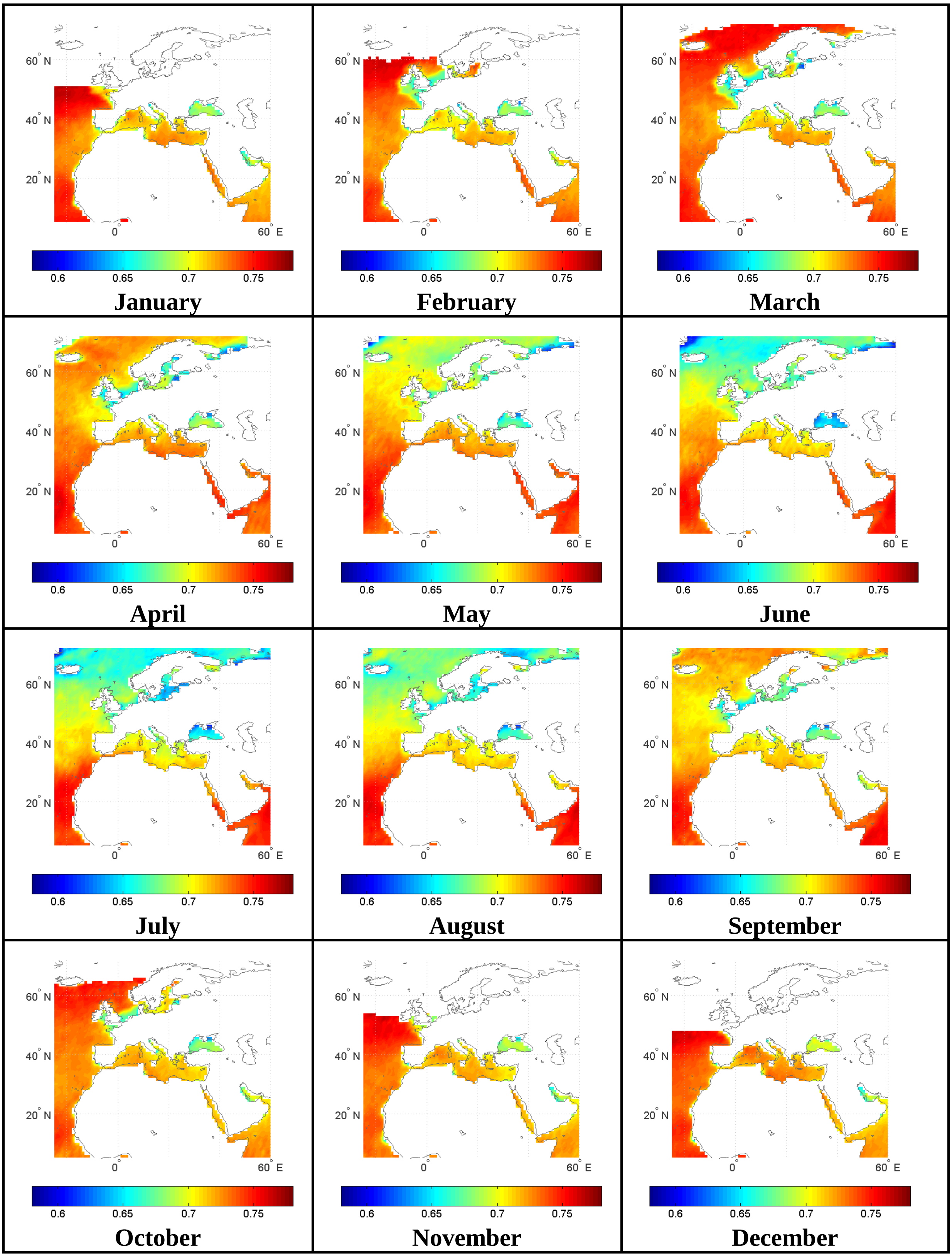

Figure 3. Month by month variation of MODIS-Aqua g_{aer} values at 470 nm averaged over the period 2002-2010.

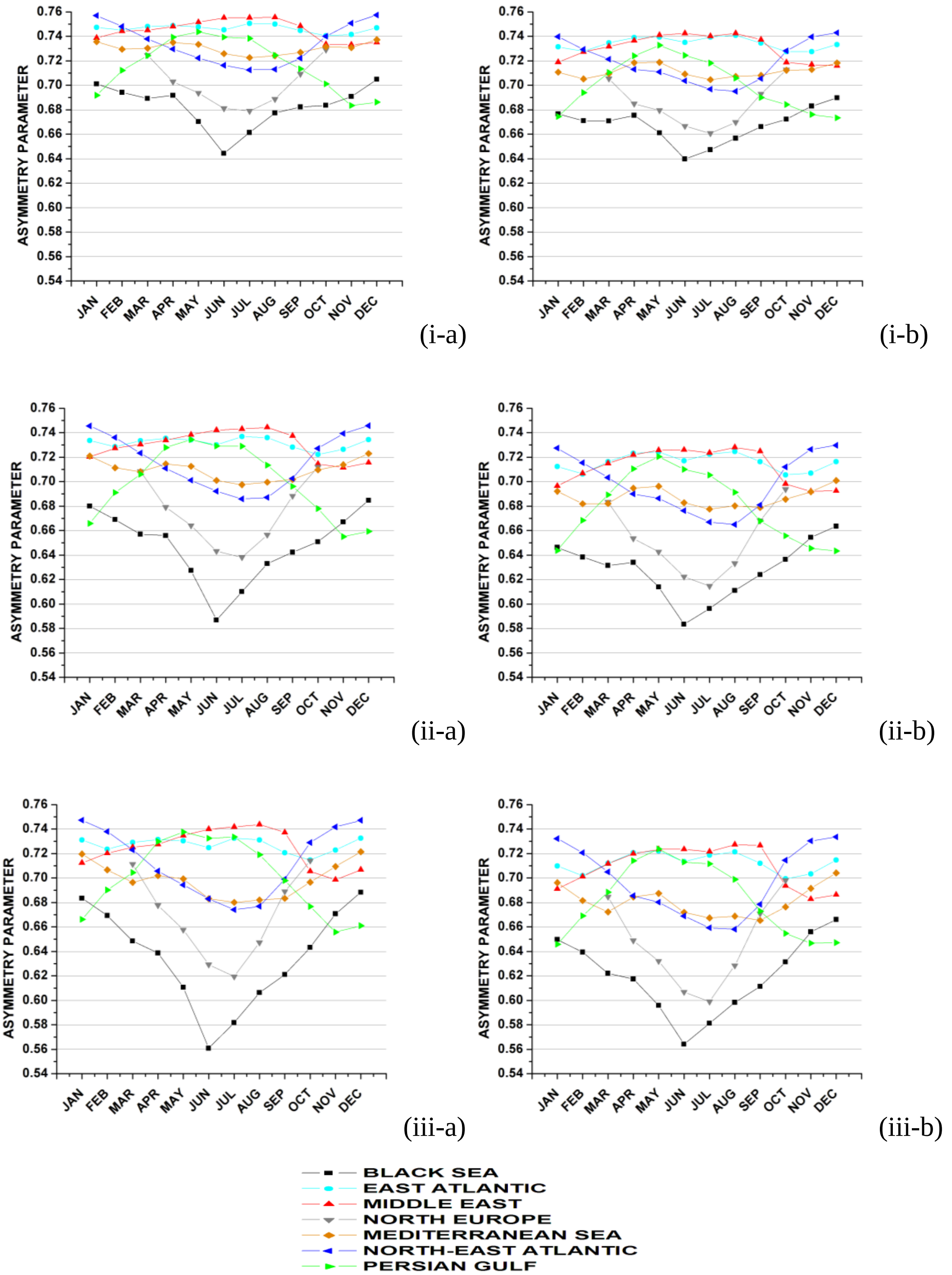

Figure 4. Intra-annual variation of MODIS Terra (-a, left column) and Aqua (-b, right column) g_{aer} values averaged over seven selected sub-regions (Fig. 1). Results are given for g_{aer} values at: 470 nm (i-, top row), 660 nm (ii-, middle row) and 870 nm (iii-, bottom row), averaged over the period 2002-2010, respectively.

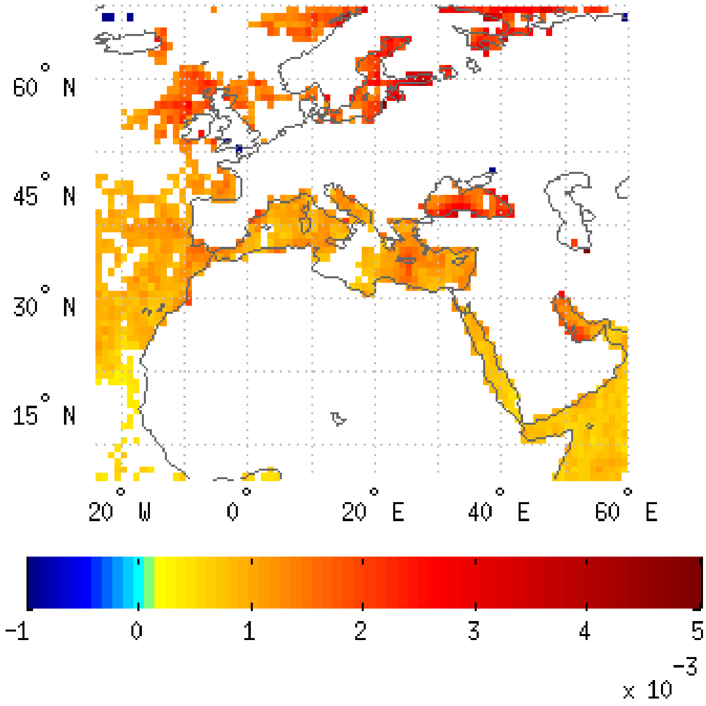

(a)

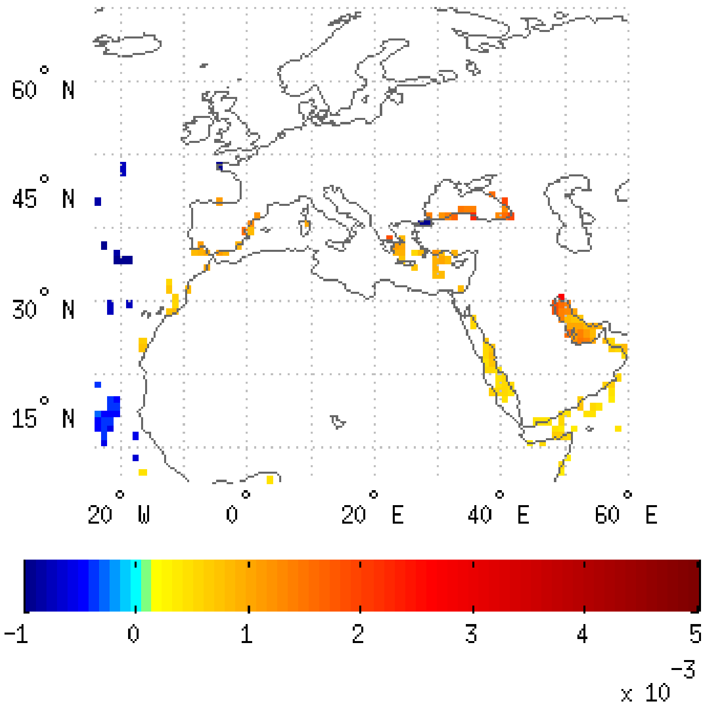

(b)

Figure 5. Slope (in units decade^{-1}) of MODIS g_{aer} deseasonalized anomalies over the period 2002-2010 from MODIS-Terra (-a, top) and MODIS-Aqua (-b, bottom), for the wavelengths of 470 nm. Results are shown only if the trend is statistically significant at the 95% confidence level.

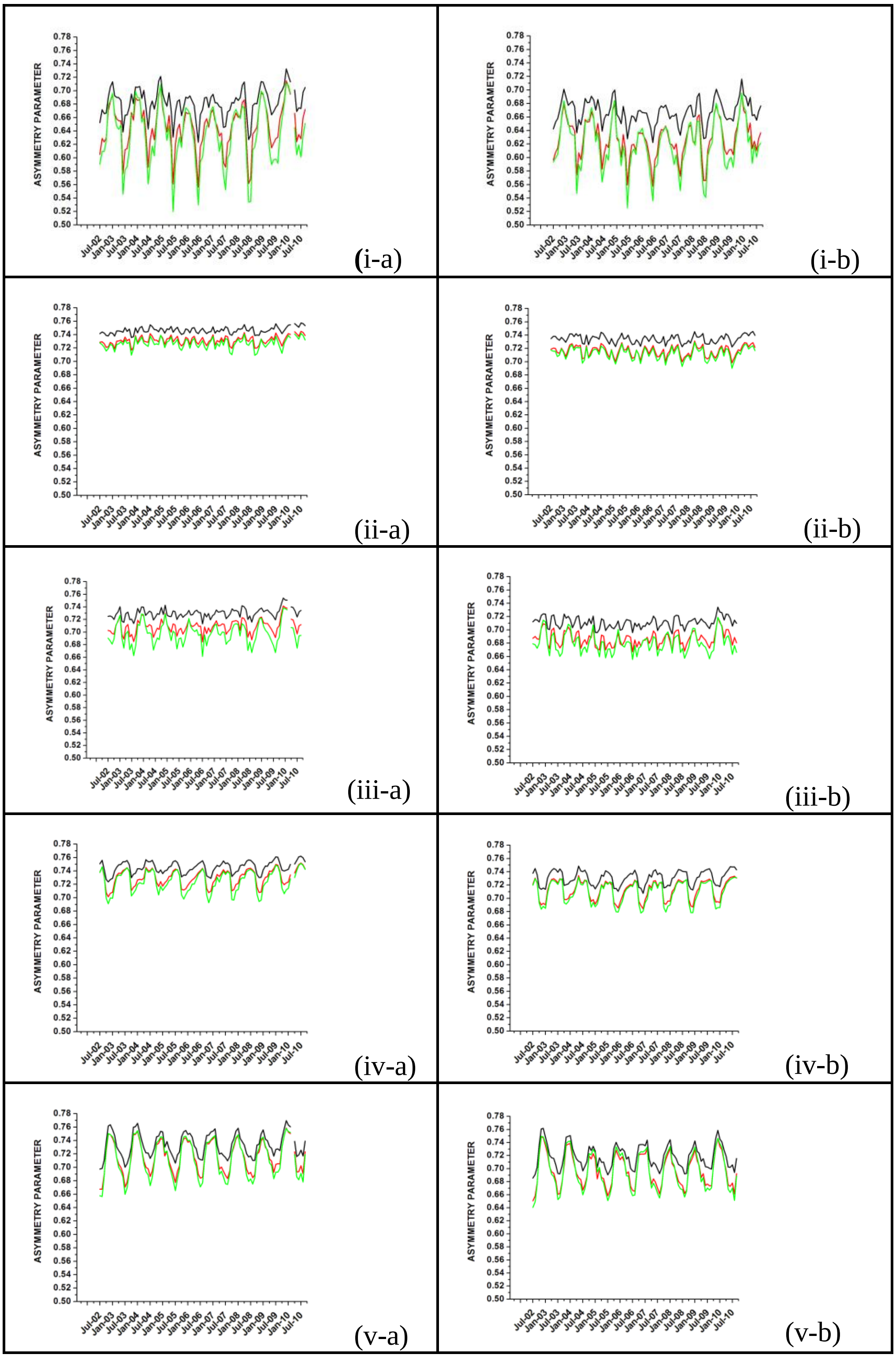

Figure 6. Inter-annual (2002-2010) variation of monthly mean g_{aer} values at 470 nm averaged over the sub-regions of: (i) Black Sea, (ii) Eastern Atlantic Ocean, (iii) Mediterranean Sea, (iv) Middle East, (v) North-eastern Atlantic Ocean, (vi) North Europe and (vii) Persian Gulf. Results are given based on MODIS-Terra (-a, left column) and MODIS-Aqua (-b, right column).

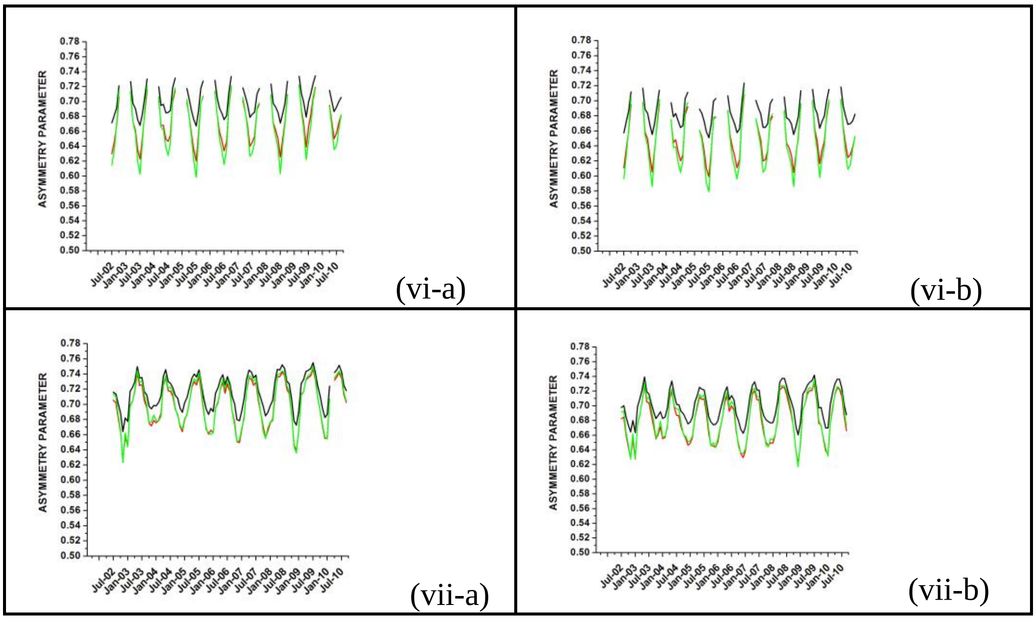

Figure 6 (continued). Inter-annual (2002-2010) variation of monthly mean g_{aer} values at 470 nm averaged over the sub-regions of: (i) Black Sea, (ii) Eastern Atlantic Ocean, (iii) Mediterranean Sea, (iv) Middle East, (v) North-eastern Atlantic Ocean, (vi) North Europe and (vii) Persian Gulf. Results are given based on MODIS-Terra (-a, left column) and MODIS-Aqua (-b, right column).

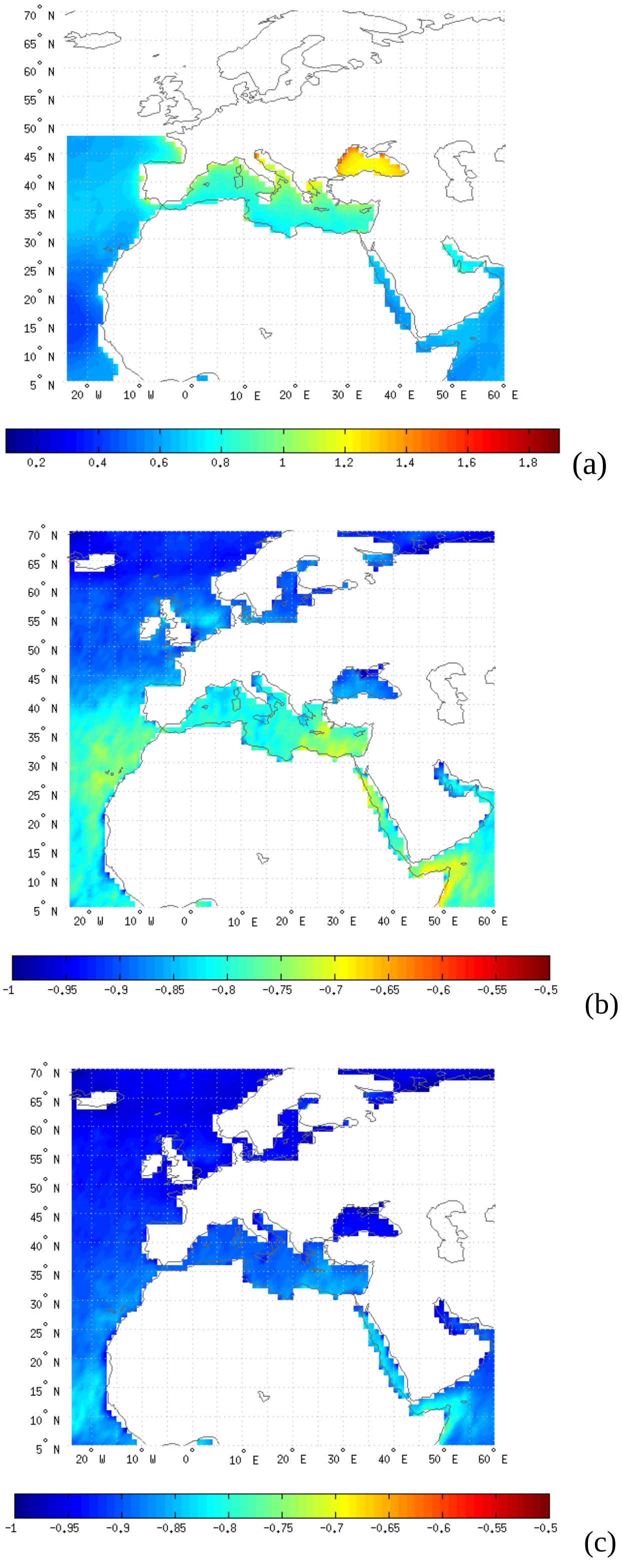

Figure 7. (a) Geographical distribution of MODIS-Aqua 051 Ångström exponent ($AE_{550-865}$) values averaged over 2002-2010, at the wavelength pair of 550-865nm. Winter AE data are missing from the northernmost areas and therefore the long-term averages in (a) are left blank. The correlation coefficients between $AE_{550-865}$ and g_{aer} data at 660 and 870 nm are given in (b) and (c), respectively.

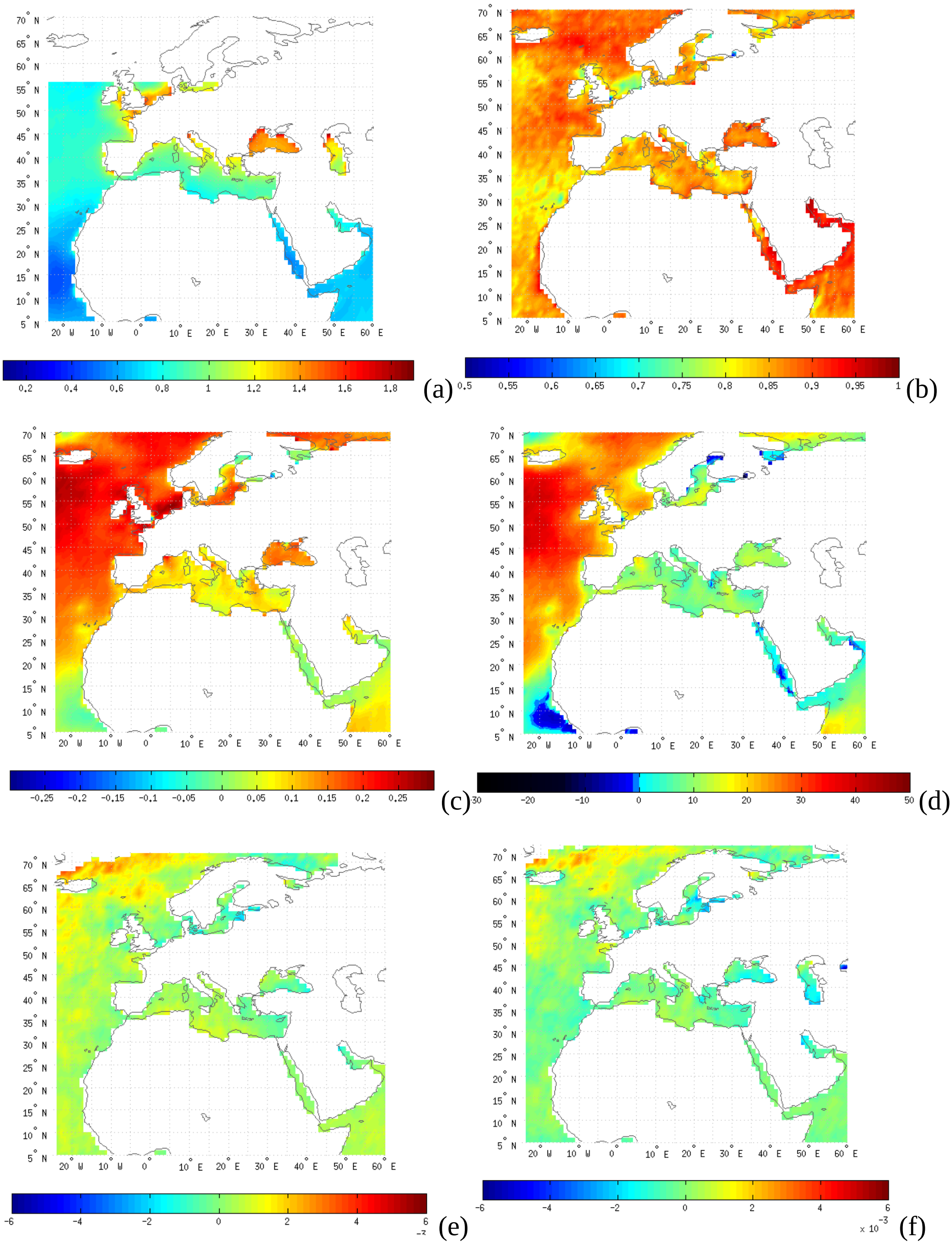

Figure 8. (a) Geographical distribution of MODIS-Aqua C006Angström exponent ($AE_{550-865}$) values averaged over 2002-2010, at the wavelength pair of 550-865nm. Winter AE data are missing from the northernmost areas and therefore the long-term averages in (a) are left blank. In (b), (c) and (d) are given the correlation coefficients, the absolute biases and the relative percent biases, respectively, between the C006 and corresponding 051 $AE_{550-865}$ data. In (e) and (f) are given the computed

deseasonalized trends of MODIS Aqua 051 and C006 $AE_{550-865}$) slope values for years 2002-2010, respectively.

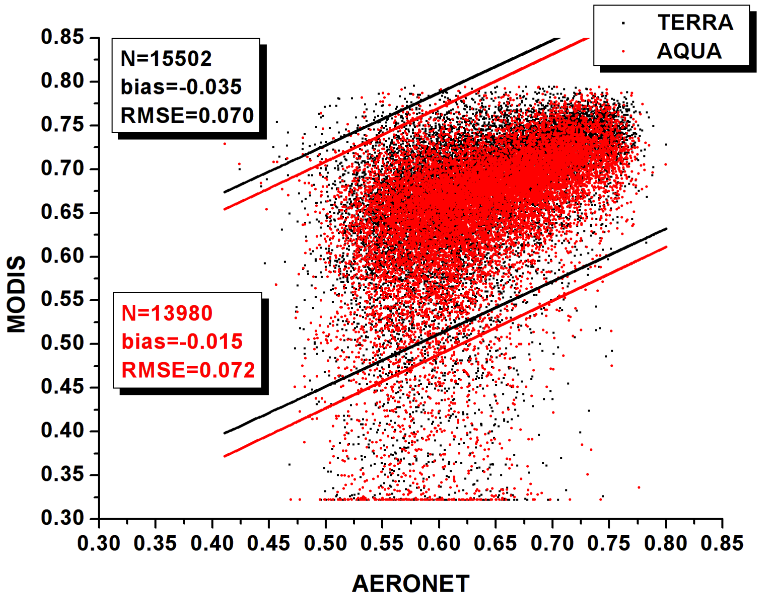

Figure 9. Scatterplot comparison between g_{aer} values at 870 nmfrom MODIS Terra (black color) and Aqua (red color) and corresponding values from AERONET stations (blue squares, Fig. 1). The 95% prediction bands as well as the mean bias (AERONET minus MODIS) and root mean squared error are given.

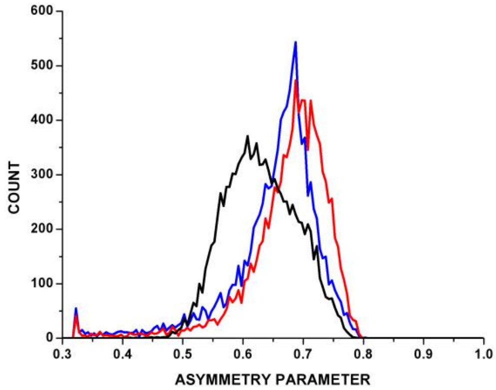

(a)

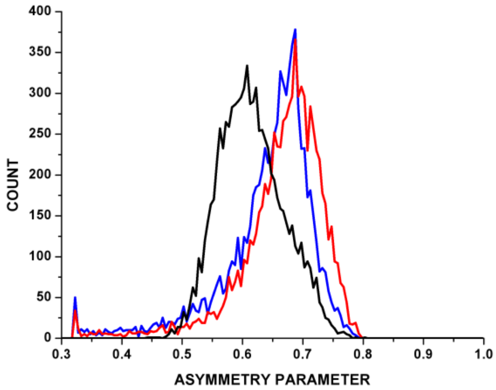

(b)

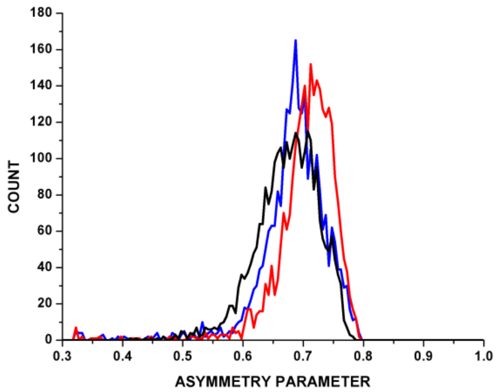

(c)

Figure 10. Frequency distribution histograms for MODIS-Terra (red colored lines) MODIS-Aqua (blue-colored lines) and AERONET (black lines) g_{aer} values at 870 nm. The histograms are given separately for: (a) the entire study region, (b) Europe and (c) Africa, Middle East and Arabian peninsula.

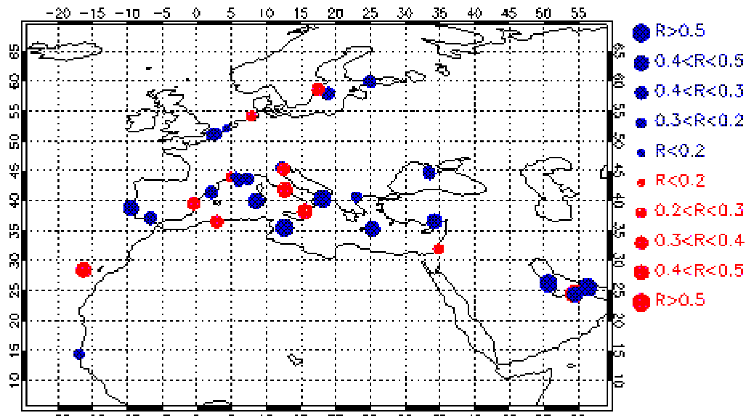

(a)

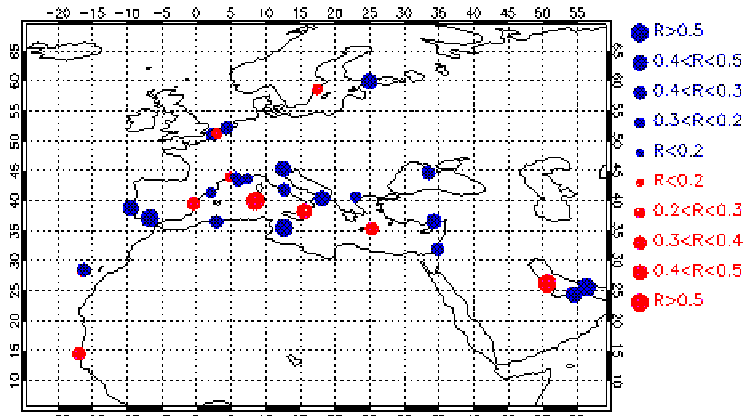

(b)

Figure 11. Map distribution of correlation coefficients between: (i) MODIS-Terra and AERONET g_{aer} values at 870 nm (left column) and (ii) MODIS-Aqua and AERONET g_{aer} values at 870 nm (right column). The size of circles corresponds to the magnitude of correlation coefficients, while blue and red colors are used for stations for which MODIS and AERONET indicate same and opposite tendency of g_{aer}, respectively.